Zeitschrift: Schweizerische mineralogische und petrographische Mitteilungen = Bulletin suisse de minéralogie et pétrographie

Band: 77 (1997)

Heft: 2

Artikel: Relics of pre-Alpine ophiolites in the Serie dei Laghi (Western Southern Alps)

Autor: Giobbi Origoni, Evelina / Zappone, Alba / Boriani, Attilio

DOI: https://doi.org/10.5169/seals-58480

SCHWEIZ. MINERAL. PETROGR. MITT. 77, 187–207, 1997

Relics of pre-Alpine ophiolites in the Serie dei Laghi (Western Southern Alps)

by *Evelina Giobbi Origoni*[1], *Alba Zappone*[1], *Attilio Boriani*[1], *Rosangela Bocchio*[1] and *Lauro Morten*[2]

Abstract

Banded amphibolites with lenses of amphibolite with garnet relics, metagabbro, pyroxenite and spinel peridotite with pyroxenite veins, occur in a continuous horizon in the Serie dei Laghi, a basement unit of the western Southern Alps, which shows a lower amphibolite facies Variscan metamorphism. The chemical composition of the amphibolites is homogeneous, that of the associated metagabbros is variable; these rocks are quite similar to the MAR tholeiitic basalts and cumulitic gabbros. The pyroxenites show a wide range of composition, as many ophiolitic pyroxenites do. In the peridotites two groups are distinguished: upper mantle peridotites with restitic character (Mg# = 90), peridodites with characteristics of a mantle contaminated by melts or fluids (Mg# less than 88). T and P estimates for the pyroxenites give T > 800 °C and P around 12 kb which suggests a lower crustal environment. Amphibolites with Amph-Pl kelyphite around garnet and Di-Pl symplectite represent the products of transformation of an eclogitic assemblage and suggest even higher pressure conditions. The amphibolite facies overprint appears related to the main regional Variscan metamorphism (about 600 °C and 6–8 kb). The studied mafic and ultramafic rocks likely represent relics of an ophiolite belt. They were dispersed into turbiditic metasediments within an accretionary prism in the early stages of the Variscan cycle.

Keywords: geochemistry, ophiolite, accretionary prism, Variscan metamorphism, Serie dei Laghi, Southern Alps.

Introduction

A continuous horizon of banded amphibolites, amphibolites with garnet relics, metagabbros and ultramafic rocks occurs in the *Serie dei Laghi* (Northern Italy and Ticino Switzerland), within the Southern Alps, displaying a Variscan amphibolite facies metamorphism.

The presence of such horizons as continuous layers or just as shreds is a constant feature of the European Variscan basement. The literature on these rocks is extensive e.g. for the French Massif Central and Armorican Massif. See for example: FORESTIER, 1963; NICOLLET et al., 1979; PIN and VIELZEUF, 1988; SANTALLIER et al., 1988; BOUCHARDON et al., 1989; DOWNES et al., 1989. According to MATTE (1991) these mafic and ultramafic rocks represent remnants of oceanic rocks trapped during the closure of two oceanic basins, the Rheic in the north and the Galicia-Massif Central in the south. The closure of the two oceanic basins, by respectively southward and northward subduction-obduction which was responsible for a HP event, occurred between 500 and 380 Ma (pre-collisional stages). It was followed by intracontinental lithospheric (collisional stage) subduction which caused intermediate pressure metamorphism (380–300 Ma). The post-orogenic period (300–250 Ma) was dominated by strike-slip faulting, extension and ascent of deep crustal (or mantle) magma.

THE MASSICCIO DEI LAGHI

The Southalpine basement consists of a group of metamorphosed, mostly siliciclastic, terranes with minor intrusives. Each terrane shows a peculiar

[1] Dipartimento di Scienze della Terra, Università degli Studi di Milano, Via Botticelli 23, I-20133, Milano, Italy. Corresponding author: E. Giobbi Origoni; e-mail: giobbi@r10.terra.unimi.it
[2] Dipartimento di Scienze della Terra e Geologico Ambientali, Università degli Studi di Bologna, Piazza di Porta San Donato 1, I-40126, Bologna, Italy.

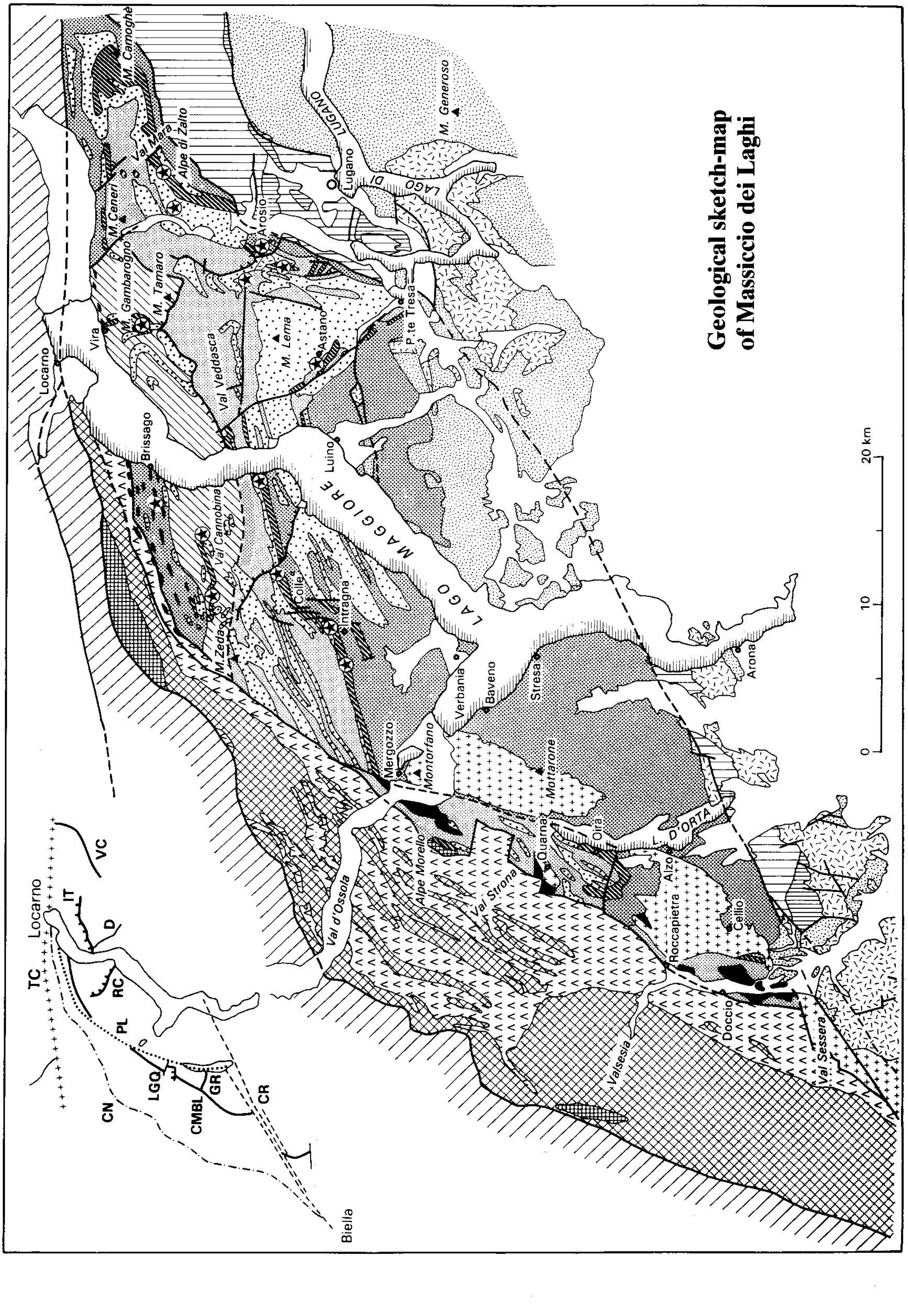
Geological sketch-map
of Massiccio dei Laghi
0
10
20 km
Locarno
Vira
Brissago
M. Gambarogno
M. Tamaro
M. Ceneri
Val Mara
Alpe di Zalto
M. Camoghè
Arosio
Lugano
LAGO DI LUGANO
M. Generoso
Val Veddasca
M. Lema
Astano
P.te Tresa
Luino
LAGO MAGGIORE
Val Cannobina
M. Zeda
Colle
Intragna
Verbania
Baveno
Stresa
Arona
Mergozzo
Montorfano
Mottarone
Val d'Ossola
Alpe Morello
Val Strona
Quarna
Oira
L. D'ORTA
Alzo
Roccapietra
Cellio
Doccio
Valsesia
Val Sessera
Biella
TC
IT
VC
D
RC
PL
LGO
GR
CR
CMBL
CN

Fig. 1 Geological sketch-map of Massiccio dei Laghi (modified after BORIANI et al., 1990a).

1 Quaternary

2 Sedimentary Mesozoic-Cainozoic cover

3 Permian volcanic rocks

4 Permian granites ("Graniti dei Laghi")

5 Permian mafic and acidic stocks and dykes ("Appinites")

VAL COLLA ZONE:

6 a b (a) Schists, phyllonites, epidote-amphibolites; (b) "Gneiss Chiari"

SERIE DEI LAGHI:

7 a b (a) Strona Ceneri Zone (paragneisses, including Cenerigneisses and Gneiss minuti);
(b) Strona Ceneri Border Zone (mostly metabasites and subordinate ultramafites)

8 Scisti dei Laghi (micaschists, paragneisses)

9 Monte Riga and Gambarogno Zone: Strona Ceneri and Scisti dei Laghi rocks with complex deformation

10 Ordovician metagranitoids

IVREA VERBANO ZONE:

11 a b (a) Basic rocks, includes both granulite and amphibolite facies; (b) ultramafites

12 Kinzigites (pelitic and semipelitic, high-grade metasedimentary rocks, with subordinate marble and amphibolite intercalations)

13 ALPINE DOMAIN

14 FAULTS. In the inset: CN = Canavese; TC = Tonale-Centovalli; CMBL = Cossato - Mergozzo - Brissago; GR = Grottaccio; PL = Pogallo-Lago d'Orta; CR = Cremosina; D = Val Dumentina; VC = Val Colla

15 OVERTHRUSTS. In the inset: RC = Riale di Cannero; IT = Indemini - Monte Tamaro; LGQ = Val Lessa, Germagno and Quarna

16 Location of the analyzed samples

Location of the analyzed samples

Pyroxenites: LUCR1 - LUCR5b: Alpe di Zalto-Val Mara path; LDSC47: Alpe di Zalto-Val Mara path; LDSC49: Alpe di Zalto-Val Mara path, in the Val Mara debris; LRSC28 - LUCR4b: Val Mara; LUCR40: Alpe di Zalto; LDSC48: Val Mara.
Peridotites : LDSC30 - LDSC37 - LDSC65 - ML5s: Val Mara.
Garnet pyroxenite dykes: LDSC84: Cima di Lago; ML2 - ML5v Alpe di Zalto-Val Mara path.
Metagabbros : LRSC44: Alpe di Zalto-Val Mara path; MCMA31: Astano mine; ML4 - ML6: Alpe di Zalto-Val Mara path; ML8: Alpe di Zalto.
Garnet-bearing amphibolites: MCMA26 - MCMA40: Astano mine; MCMA51 - MCMA52 - MCMA53 -MCMA55: M. Gambarogno; MCMA48 - MCMA49: Val Cannobina road (W of Cannobio), Spoccia junction; EGCA2: Val Cannobina, bridge near Ponte Falmenta; SF6: N of Intragna; SF32: Cadorna road, N of Colle; SF53 N of Intragna; LRSC33 - LRSC35 - LRSC39: Alpe di Zalto, near Altari; LRSC50: Alpe di Zalto-Alpe Davrosio road; ML7: Alpe di Zalto-Val Mara path.
Banded amphibolites: MCMA16: Cademario; MCMA20: Arosio ; MCMA32: Laghetti di Astano.

Tab. 1 Whole rock analyses of selected samples of ultramafites from Strona Ceneri Border Zone.

Rock type	Peridotites				Pyroxenites								Pyroxenite dykes		
Sample	LDSC30	LDSC37	LDSC65	ML5s	LUCR1	LUCR5b	LDSC47	LDSC49	LRSC28	LUCR4b	LUCR40	LDSC48	LDSC84	ML5v	ML2
SiO_2	39.27	38.14	36.19	38.19	48.07	48.02	47.92	47.80	49.77	46.80	49.20	44.77	40.53	44.80	44.52
TiO_2	0.15	0.06	0.51	0.11	0.37	0.35	0.30	0.54	0.46	0.28	0.47	0.37	0.31	0.35	0.30
Al_2O_3	2.13	2.53	3.42	2.11	9.88	8.61	5.35	5.80	6.92	3.31	4.88	4.79	4.34	4.67	4.37
Fe_2O_3	6.39	1.56	7.06	5.57	1.62	1.74	1.39	1.77	2.38	2.14	0.81	3.69	8.10	3.57	2.58
FeO	5.04	5.44	3.89	4.02	5.86	7.59	5.06	6.70	5.20	6.66	8.13	7.78	2.27	3.60	5.30
MnO	0.12	0.07	0.17	0.16	0.10	0.15	0.12	0.18	0.15	0.09	0.11	0.20	0.16	0.19	0.13
MgO	33.48	34.08	34.57	35.20	18.01	17.85	24.48	18.61	18.58	27.70	20.66	23.23	23.86	22.79	28.94
CaO	3.76	3.52	2.07	2.52	12.30	12.28	10.27	15.36	13.18	9.50	13.76	9.92	7.67	14.27	7.78
Na_2O	0.16	–	0.08	0.07	1.22	0.71	0.47	0.47	1.14	0.18	0.36	0.64	0.44	0.35	0.39
K_2O	–	–	–	–	0.22	0.20	0.12	–	0.20	–	0.01	0.02	0.04	–	0.04
P_2O_5	0.03	0.10	0.10	–	0.03	0.01	–	0.05	–	0.01	0.02	0.04	–	0.03	0.01
LOI	8.72	13.67	11.24	11.22	3.04	2.80	4.52	1.73	2.01	3.83	1.71	3.47	12.28	4.40	5.64
Total	99.25	99.25	99.03	99.17	100.72	100.31	100.00	99.01	99.99	100.50	100.12	98.92	100.00	99.02	100.00
FeO*	10.79	6.84	10.24	9.03	7.32	9.16	6.31	8.29	7.34	8.59	8.56	11.10	9.56	6.81	7.62
Mg#	84.72	90.49	90.20	87.45	81.46	77.68	87.40	80.03	81.88	85.22	80.64	78.89	81.68	85.67	87.16
Rb	1	1	1	1	4	1	–	31	–	–	2	3	–	1	–
Ba	16	5	12	6	–	–	27	16	79	–	–	52	53	17	44
Sr	24	34	19	8	237	76	69	25	127	18	31	78	76	32	63
Y	4	1	5	3	7	6	7	15	12	2	5	10	8	8	7
Nb	0.12	0.33	1.92	0.21	3	5	5	0.04	5	3	2	0.27	2	0.24	4
Zr	6	7	19	7	29	22	4	9	11	17	18	6	5	8	8
Sc	19	12	12	16	n.d.	n.d.	46	43	54	n.d.	n.d.	32	43	11	39
V	128	64	107	104	320	212	303	527	544	288	361	379	392	258	228
Cr	1721	2411	2642	3943	747	1094	4882	2161	1546	3190	3320	1619	1761	6804	3183
Co	110	87	105	101	50	66	44	52	44	113	90	76	80	82	78
Ni	580	1880	1510	654	95	308	383	201	125	1350	908	274	259	751	498
Cu	35	9	19	93	51	9	n.d.	30	n.d.	6	344	68	n.d.	273	n.d.
Zn	48	39	64	57	53	54	n.d.	49	n.d.	4	25	64	n.d.	83	n.d.
Pb	3	n.d.	n.d.	6	n.d.	n.d.	n.d.	3	n.d.	n.d.	n.d.	6	n.d.	130	n.d.
Th	1.68	0.14	0.12	1.96	n.d.	n.d.	n.d.	–	n.d.	n.d.	n.d.	0.08	n.d.	0.11	n.d.
U	0.18	n.d.	n.d.	0.15	n.d.	n.d.	n.d.	0.02	n.d.	n.d.	n.d.	0.12	n.d.	–	n.d.

Major oxides in wt%, trace elements in ppm. Mg# = $(Mg/Mg + Fe_{tot}) \cdot 100$; n.d. = not determined; – = traces; FeO* = total iron as FeO.

Tab. 2 Whole rock chemistry of selected samples of metabasites of Strona Ceneri Border Zone.

Rock type	Metagabbros					Amphibolites with garnet relics								Banded amphibolites		
Sample	LRSC44	MCMA31	ML4	ML6	ML8	MCMA26	MCMA53	MCMA55	MCMA48	EGCA2	SF6	SF32	SF53	MCMA16	MCMA20	MCMA32
SiO_2	54.68	49.55	47.27	47.47	47.24	49.27	49.86	49.35	51.33	50.66	48.22	48.28	48.55	50.20	54.34	56.10
TiO_2	0.65	0.30	0.12	0.48	0.16	1.63	1.20	1.33	0.97	1.02	2.01	3.31	1.63	0.65	0.53	0.36
Al_2O_3	17.98	7.01	18.89	17.58	16.09	14.35	15.34	15.19	10.92	19.11	14.27	12.39	16.72	13.08	15.60	16.27
Fe_2O_3	1.12	2.91	1.29	1.05	1.45	1.91	1.27	1.28	6.37	1.20	2.00	3.00	1.51	2.08	2.40	1.67
FeO	4.76	8.65	7.27	7.17	5.42	10.01	9.40	9.30	6.76	6.90	10.11	12.20	9.04	6.85	4.65	6.41
MnO	0.08	0.18	0.16	0.14	0.11	0.18	0.18	0.16	0.23	0.13	0.16	0.19	0.15	0.15	0.12	0.14
MgO	5.51	17.97	8.82	9.14	15.16	6.25	6.76	6.09	8.41	5.17	8.16	7.52	6.71	11.48	7.18	5.16
CaO	8.31	7.17	9.71	11.46	10.24	10.31	11.82	12.49	10.08	9.13	9.43	9.29	10.20	8.97	8.12	8.19
Na_2O	4.62	0.49	2.84	2.16	1.84	3.07	2.33	2.55	0.74	4.32	1.66	1.43	2.54	2.41	3.60	3.35
K_2O	0.35	0.57	0.28	0.18	0.16	0.44	0.55	0.41	1.30	0.17	1.48	0.47	0.57	0.77	0.42	0.54
P_2O_5	0.07	0.05	0.05	0.06	–	0.21	0.16	0.18	0.11	0.16	0.37	0.71	0.28	0.15	0.14	0.06
LOI	1.13	4.66	2.37	1.88	2.13	1.07	1.63	0.46	1.93	1.56	1.04	1.10	1.12	2.61	2.03	1.56
Total	99.26	99.51	99.07	98.77	100.00	98.70	100.50	98.79	99.15	99.53	98.91	99.89	99.02	99.40	99.13	99.81
FeO*	5.77	11.27	8.43	8.11	6.72	11.73	10.54	10.45	12.49	7.98	11.91	14.90	10.40	8.72	6.81	7.91
Mg#	63.03	74.00	65.11	66.77	80.10	48.73	53.35	50.96	54.56	53.61	54.99	47.37	53.51	70.14	65.29	53.77
Rb	7	42	11	7	–	13	11	7	89	1	57	11	19	30	12	14
Ba	245	121	106	57	35	192	81	39	64	161	271	191	187	208	82	119
Sr	483	80	275	178	161	249	131	140	169	908	234	185	398	292	438	182
Y	12	15	12	12	3	35	23	31	23	21	27	33	24	18	18	17
Nb	0.61	1.00	0.12	0.01	2.00	5.05	3.00	2.22	2	–	17	27	12	1	1	16
Zr	30	29	–	9	1	136	63	87	47	67	126	159	105	64	58	39
Sc	17	n.d.	11	25	27	28	n.d.	27	n.d.	23	37	44	34	n.d.	n.d.	n.d.
V	149	320	40	205	118	316	286	288	302	203	266	271	272	203	156	216
Cr	314	494	31	97	416	157	262	301	189	77	208	165	153	459	242	104
Co	25	39	41	43	55	38	41	38	40	31	47	56	42	35	25	26
Ni	71	124	51	43	105	22	82	83	58	33	64	118	69	170	82	33
Cu	34	65	5	309	n.d.	27	57	61	16	22	51	70	21	24	11	94
Zn	65	130	58	51	n.d.	99	81	86	111	82	115	141	100	88	75	64
Pb	5	2	5	2	n.d.	5	1	2	2	n.d.	n.d.	n.d.	1	5	1	1
Th	0.13	n.d.	–	–	n.d.	0.66	n.d.	0.09	n.d.	10	n.d.	n.d.	n.d.	n.d.	n.d.	n.d.
U	0.17	n.d.	0.10	0.21	n.d.	0.56	n.d.	0.01	n.d.	n.d.	n.d.	n.d.	n.d.	n.d.	n.d.	n.d.

Major oxides in wt%, trace elements in ppm. Mg # = (Mg/Mg + Fe_{tot}) · 100; n.d. = not determined; – = traces; FeO* = total iron as FeO.

lithological association that can be tentatively traced back to a specific geotectonic environment and to its evolution in time .

Massiccio dei Laghi (Fig. 1) includes the two westernmost of these terranes: the *Ivrea Verbano Zone* and the *Serie dei Laghi.* These two units are separated by a system of ductile faults, the most important of which is the *Cossato-Mergozzo-Brissago Line* (BORIANI et al., 1990a).

The *Ivrea Verbano Zone* is composed of high grade metapelites, marbles, amphibolites and mafic granulites with peridotite lenses. A 10 km thick, predominantly mafic, igneous complex is also present. The HT amphibolite and granulite facies event occurred during the early Permian. It was induced by the intrusion of the mafic complex (VOSHAGE et al., 1990; VAVRA et al., 1996).

The *Serie dei Laghi* consists of lower amphibolite facies rocks which can be divided into two different subunits: the *Scisti dei Laghi* which is dominantly metapelitic, and the *Strona Ceneri* which is dominantly metapsammitic. Near the boundary with Scisti dei Laghi the Strona Ceneri is rich in mafic and ultramafic rocks (*Strona Ceneri Border Zone*). The minimum age of the metamorphic climax in Serie dei Laghi is about 320 Ma (BORIANI et al., 1990b).

The stratigraphic sequence of Serie dei Laghi can be reconstructed with some confidence. The youngest part seems to be represented by *Gneiss Minuti* which is a finely layered and graded meta-arenite sequence. A rather continuous layer of *Cenerigneiss* is present below the Gneiss Minuti. Cenerigneiss is a coarse sandy meta-conglomerate without any layering or graded bedding. The Strona Ceneri Border Zone lies below Cenerigneiss. This zone is composed of strongly layered and graded metasediments which range in composition from metabasite to metapelite; it also contains abundant ophiolitic material. *Scisti dei Laghi*, a monotonous metapelitic unit lies below the Strona Ceneri Border Zone. The attribution of Scisti dei Laghi to the same sedimentary sequence of the Strona Ceneri is questionable. A polymetamorphic history has also been proposed for this subunit (see BORIANI et al., 1990b). Lenses of *Ordovician metagranites*, which are mostly granodioritic and granitic, occur in all parts of Serie dei Laghi, but are primarily concentrated in Strona Ceneri Border Zone (BORIANI et al., 1995).

The Serie dei Laghi is folded by large folds with variable axial plunges, the largest of which is a synform with hinge at M. Camoghè, in Ticino (Switzerland), whose axial plane can be traced to the SW for about 50 kilometers. It is interpreted as a syncline with the Gneiss Minuti in its core. The main foliation lies in the axial plane of this fold (F1). F2 folds ("Schlingenbau") appear near the contact with the Ivrea Verbano Zone. F2 folds show steep axes and a weak axial plane crenulation cleavage. W of Cannobio, these folds become tighter near the Ivrea Verbano Zone where they grade into a thick shear zone characterized by strong boudinage of the more competent intercalations. This shear zone is also characterized by the presence of a subvertical belt of mylonites belonging to the *Cossato Mergozzo Brissago Line.* Schlingenbau (probably sheath folds), shear zone and mylonites are interpreted as the result of late Variscan movements at the contact between Serie dei Laghi and Ivrea Verbano Zone (BORIANI et al., 1990a), with an important horizontal component, at least in terms of present day geometry.

A mafic dyke swarm consisting of small stocks and dykes ("Appinites") is intruded in both Ivrea Verbano Zone and Serie dei Laghi along the Cossato Mergozzo Brissago Line. Between Val d'Ossola and Valsesia, the Serie dei Laghi rocks are migmatitic in a belt 1–3 km wide near Cossato Mergozzo Brissago Line. Early Permian granite plutons are aligned immediately south of the Cossato Mergozzo Brissago Line *(Graniti dei Laghi).* Further south, the basement is covered by acidic volcanic rocks of Early Permian age, which are overlain by Mesozoic sedimentary rocks.

STRONA CENERI BORDER ZONE

In the less deformed southern limb of the main F1 fold, the Strona Ceneri Border Zone has a thickness of up to 500 m. Schists, paragneisses, quartzites and banded amphibolites (that recall the LAG – Leptino-Amphibolite Group of the French Massif Central: FORESTIER, 1963), are repeatedly interlayered. Graded bedding is still visible despite the effect of regional metamorphism. Lenses of metagabbro, garnet-bearing amphibolite, peridotite, pyroxenite and serpentinite are present almost everywhere along the horizon, but are particularly abundant on the western shore of Lago d'Orta and north of Lugano.

In the strongly deformed northern part of Serie dei Laghi, the Strona Ceneri Border Zone is more discontinuous as the competent layers are boudinaged. The two most important occurrences are at M. Gambarogno (garnet-bearing amphibolite enclosed in the orthogneisses) and at Alpe Morello (symplectitic garnet-bearing amphibolites associated to a peridotite body).

The metabasite horizon of Strona Ceneri Border Zone can be divided into several different segments, each of them with a specific lithologic association.

Tab. 3 Rare earth element content of selected samples of ultramafites and metabasites from Strona Ceneri Border Zone.

Rock type	Peridotite				Pyroxenites	
Sample	LDSC30	LDSC37	LDSC65	ML5s	LDSC49	LDSC48
La	0.58	1.07	1.07	0.29	0.38	0.51
Ce	0.51	2.15	3.38	0.88	0.10	1.03
Pr	0.21	0.28	0.53	0.15	0.39	0.34
Nd	1.04	1.30	2.56	0.10	2.69	2.09
Sm	0.38	n.d.	n.d.	0.25	1.24	0.89
Eu	0.15	0.08	0.31	0.11	0.47	0.37
Gd	0.46	0.21	0.94	0.38	1.61	1.05
Tb	0.11	0.04	0.15	0.07	0.35	0.25
Dy	0.68	0.26	0.88	0.46	2.42	1.54
Ho	0.15	0.05	0.19	0.11	0.60	0.40
Er	0.41	0.12	0.41	0.24	1.57	1.03
Tm	0.06	0.02	0.06	0.03	0.23	0.15
Yb	0.40	0.17	0.38	0.23	1.47	0.93
Lu	0.06	0.02	0.06	0.04	0.24	0.14
Rock type	Pyroxenite dyke	Metagabbros			Amphibolites with garnet relicts	
Sample	ML5v	LRSC44	ML4	ML6	MCMA26	MCMA55
La	0.51	1.94	1.02	0.58	7.41	3.43
Ce	1.90	4.30	2.20	1.82	18.59	9.36
Pr	0.33	0.83	0.28	0.33	2.92	1.63
Nd	2.12	4.57	1.31	2.15	14.47	9.14
Sm	0.90	1.62	0.36	1.06	4.36	3.20
Eu	0.35	0.88	0.75	0.54	1.62	1.22
Gd	0.94	1.58	0.30	1.30	4.50	3.47
Tb	0.18	0.33	0.05	0.27	0.89	0.76
Dy	1.39	1.90	0.26	1.84	5.52	4.81
Ho	0.34	0.48	0.06	0.44	1.38	1.27
Er	0.81	1.22	0.15	1.08	3.66	3.34
Tm	0.12	0.18	0.02	0.18	0.54	0.52
Yb	0.75	1.10	0.17	1.12	3.38	3.09
Lu	0.12	0.17	0.04	0.17	0.53	0.50

Tab. 4 Selected microprobe analyses of olivine of Strona Ceneri Border Zone.

Rock type	Peridotite	Pyroxenites			
Sample	ML5s	LUCR40 p4f6	LUCR4B	DSC49	LDSC47
SiO_2	39.52	38.65	39.42	38.38	38.74
TiO_2	0.01	0.02	0.00	0.00	0.01
FeO	14.06	21.19	19.29	20.85	20.40
MnO	0.20	0.26	0.21	n.d.	n.d.
MgO	46.08	40.84	42.60	41.48	40.94
NiO	0.10	n.d.	n.d.	0.09	0.02
CaO	0.01	0.04	0.06	0.02	0.01
Tot.	99.98	101.00	101.58	100.82	100.13
Si	0.986	0.987	0.991	0.978	0.995
Ti	0.000	0.000	0.000	0.000	0.000
Fe^{2+}	0.293	0.453	0.406	0.444	0.438
Mn	0.004	0.006	0.005		
Mg	1.714	1.555	1.597	1.575	1.567
Ni	0.002			0.002	0.000
Ca	0.000	0.000	0.002	0.001	0.000
Forsterite	0.85	0.77	0.80	0.80	0.78
Fayalite	0.15	0.23	0.20	0.22	0.22
Tephroite	0.00	0.00	0.00	0.00	0.00

n. d. = not determined
Structural formulae on the basis of 3 cations.

1) In the southwestern part, between Valsesia and Lago d'Orta, the ultramafic rocks are rather abundant. A small lens of serpentinite occurs near Cellio (Valsesia) within the contact aureole of the Alzo-Roccapietra granite. A 300 m long and 100 m thick subvertical serpentinite lens, occurs in the amphibolite horizon at Oira (western shore of Lago d'Orta).

2) Between Val d'Ossola (Mergozzo) and the Dumentina fault (eastern shore of Lago Maggiore), the ultramafites are absent and the metabasites maintain homogeneous features for several kilometers. Two type sections were studied in detail: the first one at Ponte Nivia where the metabasites reach their maximum thickness. The second one, thinner than the former, lies north of Maccagno very close to the Dumentina fault. In both sections the amphibolites preserve premetamorphic grain-size variations and compositional banding, generally transposed in the main foliation. Thin intercalations of metapelite, sometimes containing large garnets, staurolite and kyanite, or metagraywacke and metaquartzite are also present. The compositional banding is either gradational or sharp, and due to extreme variability of the protolith, which could have been a sequence of basaltic tuffites, arenites with volcanic clasts and pelites. Very often the banded amphibolites grade into amphibolites with K-feldspar augens, whose size and distribution seems related to the banded texture of the amphibolites. Streaks of small augens appear in the finer grained varieties, while large crystals, up to 10 cm in length, appear in the coarser grained types. The type sections of P.te Nivia and Maccagno were described by Boriani and Giobbi Mancini, 1972 and by Giobbi Origoni et al., 1982/83, respectively.

Garnet-bearing amphibolites are found as thin discontinuous lenses along the horizon. Isolated lenses of metagabbro, rarely exceeding 1 meter in length, are sometimes present.

3) From Maccagno to Val Vedeggio the metabasite horizon, which is divided into segments by a system of subvertical N–S brittle faults of prob-

able Alpine age, is dominated by the banded amphibolites. One of the most interesting outcrops is the abandoned Astano mine (Fe, Cu, Zn and Pb sulfides). A detailed description was given by KELTERBORN (1923) and GRAETER (1951).

4) From Val Vedeggio to M. Camoghè, ultramafite bodies, tens to hundreds of meters long, are very abundant. Amphibolites with garnet relics are found as layers in the banded amphibolites or as xenoliths in the ortogneisses. Lenses of metagabbro, displaying a flaser texture, are present in the fine grained amphibolites and in the ultramafites. K-feldspar-bearing amphibolites are rare. The ultramafic lenses are intensely serpentinized at the contact with the metapelites of the Strona Ceneri Border Zone. The relationships among peridotite, pyroxenite and metagabbro can be studied along the Val Mara–Alpe di Zalto footpath in Val d'Isone (SPICHER, 1940). Boudins of pyroxenite dykes, a few dm thick, can be followed for more than one hundred meters in the peridotite body. Locally, the ultramafites also contain small boudins of amphibolites with garnet relics.

5) In the northern part of Serie dei Laghi the metabasite horizon is less continuous. Small boudins of amphibolite with garnet relics occur in the schists along the Insubric Line and in the orthogneisses of M. Gambarogno. Discontinuous and folded layers of banded amphibolites occur W of Cannobio. These banded amphibolites contain small lenses of intensely altered ultramafic rocks (*Strahlsteinfelse*, SPICHER, 1940) and lenses of amphibolites with garnet relics. Further SW, west of the Pogallo fault, these amphibolites reappear at M. Faiè and in the M. Cerano area, where they seem strictly connected with the ultramafic body of Alpe Morello. The Alpe Morello body consists of a partly serpentinized dunite-harzburgite with websterite veins (MARCHESI et al., 1992), a finely layered sequence of pyroxenite with different amounts of olivine, coarse pyroxenite, amphibolite with garnet relics, and banded amphibolite. The Alpe Morello body lies along the Cossato-Brissago-Mergozzo Line, which separates the Ivrea Verbano Zone from Serie del Laghi. It has usually been attributed to the Ivrea Verbano Zone, but our field work has shown that this attribution must be revised. The samples from Alpe Morello are not considered in this paper.

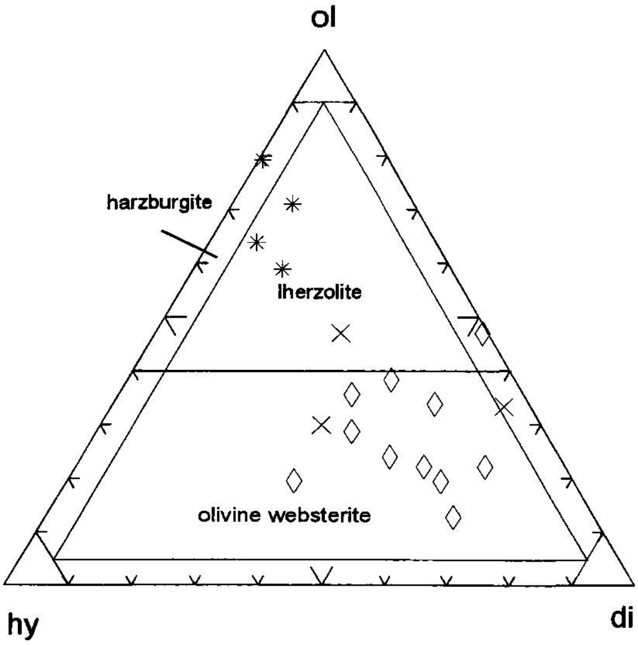

Fig. 2 Classificatory diagram of the analyzed ultramafic rocks of Strona Ceneri Border Zone according to their normative mineral content. Symbols: diamonds = pyroxenites; asterisks = peridotites; crosses = garnet pyroxenites.

Petrography and bulk rock chemistry

Tables 1 and 3 present major, minor, trace and rare earth element (REE) data of representative samples. All elements were analysed by X-ray fluorescence spectrometry, except for samples LDSC30, LDSC37, LDSC65, ML5s, LDSC49, LDSC48, ML5v, LRSC44, ML4, ML6, MCMA26; MCMA55, determined by ICP-AES and ICP-MS at CRPG (CNRS- Vandoeuvre lès Nancy, France). The FeO content was determined by potentiometric titration with $K_2Cr_2O_7$. REE analyses on selected samples were carried out at CRPG by the ICP-MS technique.

A complete chemical data set, petrographic descriptions and details on sample locations are available on request from the authors.

PETROGRAPHY OF ULTRAMAFITES

Peridotites. The peridotites of the Strona Ceneri Border Zone consist of olivine, clinopyroxene and minor orthopyroxene, amphibole (pargasite), serpentine (antigorite), chlorite (clinochlore), red-brown to black spinel and opaque ores. Olivine and pyroxenes, showing a mortar texture, are found as isolated porphyroclasts, or as flattened lenticular aggregates. Olivine is generally crosscut by fractures filled with serpentine. Orthopyroxene is almost completely altered to bastite. Where alteration is particularly developed, amphibole (pargasite), serpentine (antigorite) and chlorite (clinochlore) become the main constituents. Antigorite, which is sometimes interwoven with actinolite and subordinate chlorite, gives rise to a "mesh" texture. Diablastic porphyroblasts of clinochlore grow in the serpentine-, chlorite-, actinolite-rich matrix. In serpentinized peridotites, spinels usually show a bimodal grain size distribution. They occur as small grains in clusters in the cleavage planes of clinopyroxene or as large (up to 0.5 mm), fractured crystals at the olivine grain boundaries. More rarely they occur as rounded grains enclosed in the olivine crystals. The dominant ore-mineral is pentlandite.

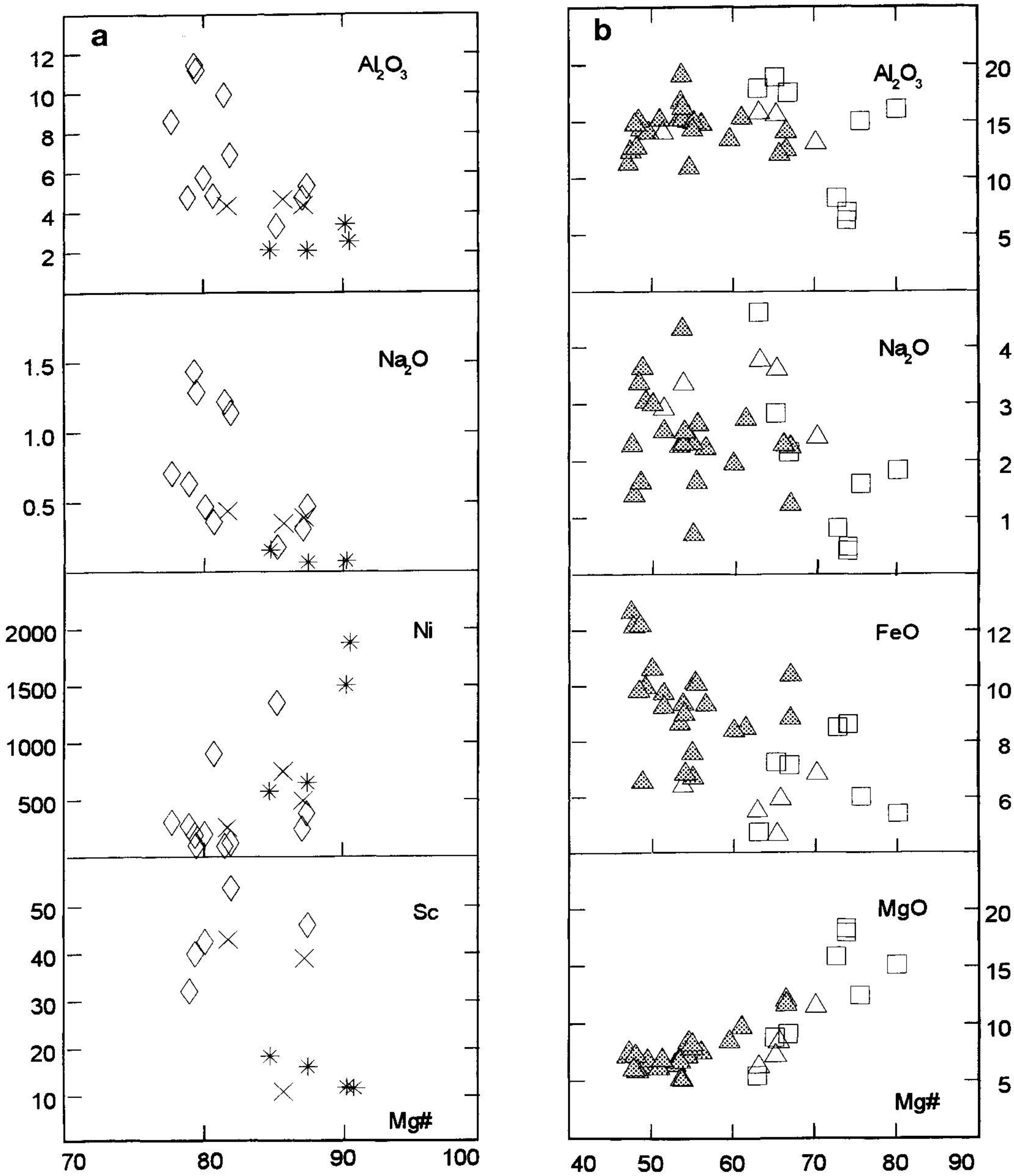

Fig 3 Major and trace elements vs Mg# variation diagrams of (a) Strona Ceneri Border Zone ultramafites, (b) Strona Ceneri Border Zone metabasites. Symbols: squares = metagabbros; stippled triangles = amphibolites with garnet relics; open triangles = banded amphibolites; other symbols as in figure 2.

Pyroxenites. The coarse grained pyroxenites from Val Mara show a granoblastic texture with clinopyroxene, olivine and subordinate orthopyroxene being the main phases. In some samples a cumulitic texture is still preserved. Clinopyroxene crystals display very fine twinning, and occasionally kinked lamellae. Olivine and orthopyroxene are sometimes enclosed in clinopyroxene. Greenish, euhedral to sub-rounded spinel is always associated with olivine in cumulus assemblage. Grains reach a maximum size of around 0.5 mm and occur at olivine grain boundaries or, rarely, are enclosed in clinopyroxene. Mg-hornblende is present as large individuals or as needles along the cleavage in the clinopyroxenes. Chlorite (clinochlore) mainly occurs in the fine grained matrix, although it also forms diablastic porphyroblasts. This mineral shows polysynthetic twinning.

Large garnet grains are only present and abundant in the small pyroxenite boudins (ML2) within the peridotite body, particularly at their rims.

The smallest lenses of ultramafic rocks are sometimes completely altered to an aggregate of radial needles of pale green amphibole and chlorite ("Strahlsteinfelse").

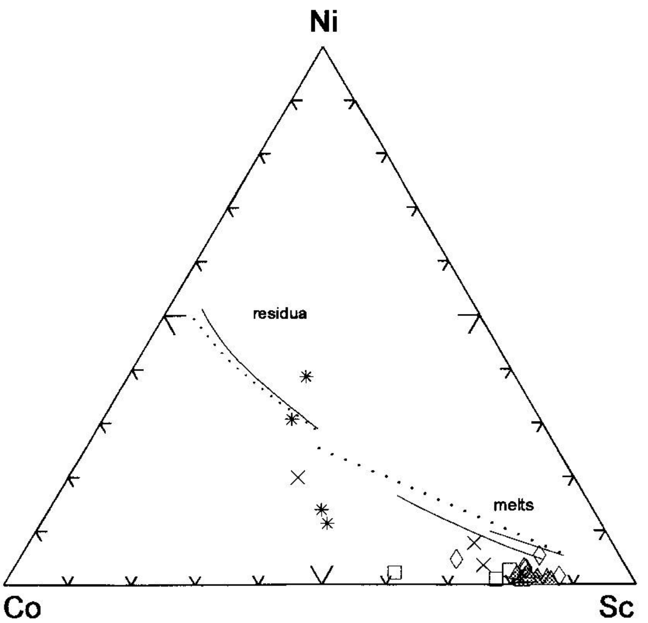

Fig. 4 Co–Ni–Sc distribution in ultramafites and metabasites of Strona Ceneri Border Zone. Trends for equilibrium melting (solid lines) and fractional melting (dotted lines) of a spinel peridotite are after OTTONELLO et al., 1984. Samples are plotted after normalization to primitive mantle abundances (JAGOUTZ et al., 1979): Symbols as in figures 2–3.

GEOCHEMISTRY OF ULTRAMAFITES

On the basis of the normative composition, the peridotites may be classified as olivine-rich and clinopyroxene-poor lherzolites and the pyroxenites may be termed olivine-websterites; the latter show a trend of decreasing diopside at a fairly similar olivine/hyperstene ratio (Fig. 2).

The peridotites show different Mg#, i.e. two have Mg# = 90 and fall in the Mg# 88–92 range considered the normal interval of the upper man-

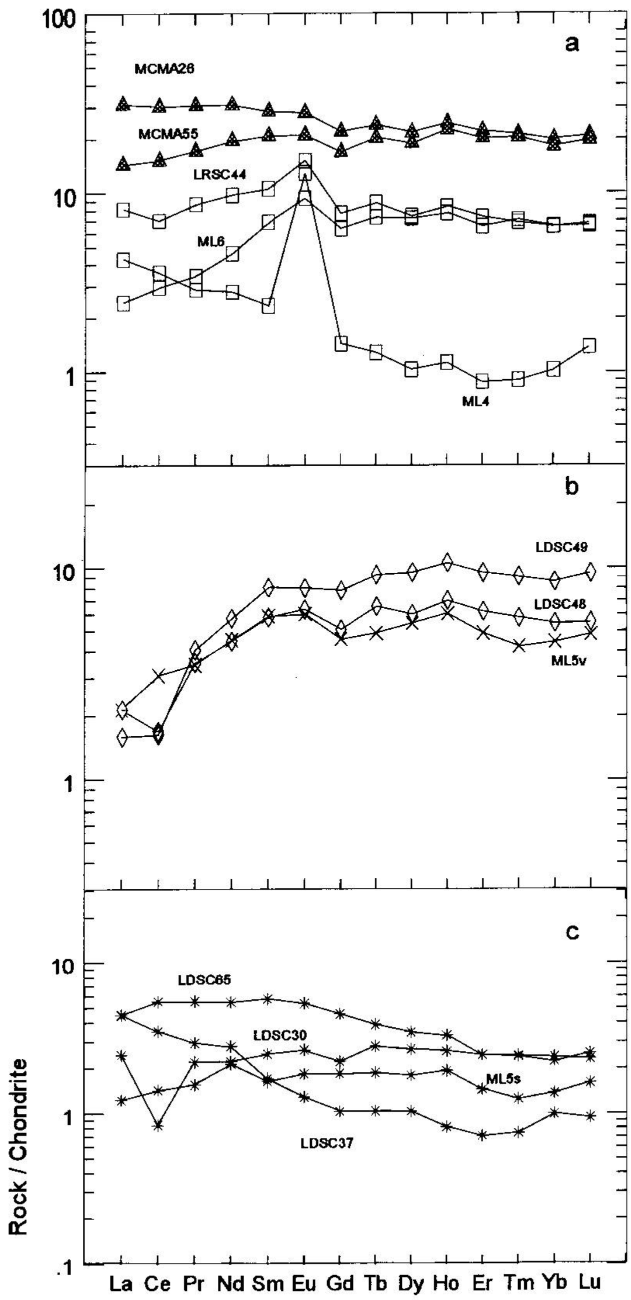

Fig. 5 Chondrite-normalized REE patterns: (a) amphibolites with garnet relics and metagabbros; (b) pyroxenites; (c) peridotites. Normalization after SUN and MCDONOUGH, 1989. Symbols as in figures 2–3.

tle material, the other two have Mg# < 88, respectively Mg# 87 and Mg# 84. These are similar to those of the Fe-rich xenolith suite, considered to represent compositional heterogeneity of the upper mantle (WILKINSON and BINNS, 1977; MORTEN, 1987) and to the iron-rich cumulitic peridotites of the Lower Layered Group of the Balmuccia body (RIVALENTI et al., 1975; 1980). The peridotites with Mg# < 88 contain less normative olivine and are slightly enriched in pyroxene. The chemical composition of the two types of peridotites is quite similar except for the Ni and Sc contents (Tab. 1 and Fig. 3a). In the Ni–Co–Sc diagram (Fig. 4) the peridotites with Mg# = 90 plot very close to the field of mantle peridotites with slightly residual character, since fractional and equilibrium melting of a peridotite source drive the residua towards the Sc-poor region at a roughly constant Ni/Co ratio (OTTONELLO et al., 1984). The peridotites with Mg# < 88 plot outside any possible trends of residua and/or extracted melts: this suggests a contamination by melt and/or fluid components (MORTEN, 1987).

The peridotites with Mg# < 88 show nearly flat REE patterns (Fig. 5c), about two times chondrites (SUN and MCDONOUGH, 1989), comparable with those of some peridotites from the Western Alps (OTTONELLO et al., 1984). The peridotites with Mg# = 90 have REE distribution patterns with slight enrichment LREE, i.e. the La_N/Yb_N ratios are 2.0 and 4.5, respectively. These facts, coupled with the Ni and Sc behaviour, suggest that a possible metasomatic olivine-consuming and clinopyroxene-forming process affected the peridotites.

The pyroxenites show a rather wide range of chemical composition (Tab. 1 and Figs 2 and 3a) depending on the variable mineralogy and modal composition. Their CaO content ranges from 7.6 to 16 wt% and spans almost all the entire range from the pyroxenites of the peridotitic orogenic massifs to ophiolitic pyroxenites (fide BEDINI, 1995). Some of the Strona Ceneri Border Zone pyroxenites have low Na_2O and moderately low TiO_2 contents similar to the ophiolitic pyroxenites; others display more alkaline character (higher Na_2O and TiO_2 content, see Tab. 1). In addition the Ni–Co–Sc behaviour indicates derivation from early extracted melts and different percentages of melting (Fig. 4).

The pyroxenites have REE contents from 1 to 10 times chondrites and are LREE depleted. The REE patterns show a positive slope from LREE to MREE and are nearly flat from MREE to HREE (Fig. 5b). Such REE behaviour is characteristic of pyroxenite segregates crystallized from tholeiitic melts (SUEN and FREY, 1987).

PETROGRAPHY OF METABASITES

Metagabbros. The metagabbros usually display a coarse-grained flaser texture. Despite the metamorphic overprint, a primary igneous cumulitic texture is still preserved. Plagioclase is generally zoned, with a highly saussuritized core surrounded by clouds of not identified minerals which in turn are rimmed by a corona of plagioclase. A few crystals are twinned, according to the albite or albite-pericline laws with deformed, discontinuous lamellae. Plagioclase occurs also as small crystals forming leucocratic layers often with polygonal texture. Idiotopic aggregates of small grains of pale green amphibole have completely replaced the primary pyroxene.

Amphibolites with garnet relics. The amphibolites with garnet relics display a very peculiar texture. Amphibole and plagioclase form tiny vermicular symplectites. In place of amphibole, diopside is sometimes found in the symplectitic intergrowths. Garnet relics are more or less replaced by kelyphytic plagioclase and hornblende. In turn, the kelyphyte is surrounded by a corona of polygonal plagioclase grains. In the amphibolites that underwent an almost complete recrystallization, garnet is surrounded by a rim of polygonal plagioclase grains, while the symplectites are transformed into a granoblastic aggregate of hornblende and plagioclase. Hornblende porphyroblasts, crowded with tiny inclusions of opaque minerals, grow in the symplectitic matrix. The colour of the amphibole shows concentrically or patchy zoning from light to dark green. Rutile, ilmenite and sphene are commonly present. Rutile is often rimmed by ilmenite, sometimes with a later overgrowth of sphene.

The observed textures indicate that these rocks are polymetamorphic. They are very similar to the products of transformation in the amphibolite facies conditions of original eclogites described by many authors (see discussion in the concluding remarks).

Banded amphibolites. The fine-grained dark bands consist of hornblende and plagioclase, rare garnet, biotite and quartz arranged in a granoblastic texture; sphene and ilmenite are common accessory minerals. These amphibolites grade into more leucocratic (trondhjemitic?) bands in which polygonal plagioclase aggregates are dominant, with minor biotite, quartz and hornblende.

GEOCHEMISTRY OF METABASITES

Tables 2 and 3 show the major, trace and rare earth element data of a representative group of samples.

Metagabbros, garnet-bearing amphibolites and banded amphibolites have a basaltic compositions, i.e. SiO_2 ranges from 47 to 57 wt% (Tab. 2), with Mg# varying from 47 to 80: the metagabbros are the least fractionated among the metabasites. However, they show some variations from more mafic to the more leucocratic samples (Fig. 3b): in particular, five of them are Mg-rich while the others are Al- and Na-rich, in response to the relative abundance of cumulus minerals (i.e., clinopyroxene and plagioclase).

The metagabbros show variable REE patterns (Fig. 5a) which suggests that different phases were involved in the fractionation processes, i.e. plagioclase for sample ML4 and pyroxenes for sample LRSC44. In addition, the presence of a significant positive Eu anomaly in the Al-rich samples suggests that plagioclase crystallized as cumulus phase and played an important role in the fractionation process that produced the gabbros. In general, the REE abundances and patterns of the metagabbros and of the garnet-bearing amphibolites are similar to the MAR cumulitic gabbros and to the MAR tholeiitic rocks (KAY et al., 1970).

In the Ni–Co–Sc diagram (Fig. 4) the metabasites fall below the trends of melts extracted through both fractional and equilibrium melting.

K-feldspar bearing amphibolites. Although geochemistry and mineral chemistry of these rocks are not considered in the present study, they provide important clues for understanding the evolution of the amphibolite horizon. They contain abundant biotite, K-feldspar and quartz. These minerals are either important constituents of the rock, which then grades into a hornblende-biotite augen gneiss, or they form cm thick veins concordant with the sedimentary layering of the more fine grained amphibolites.

Field relationships, texture, mineral and chemical compositions suggest either a metasomatic feldspatization or a pre-metamorphic infiltration of residual liquids probably derived from the Ordovician granitoids (BORIANI and GIOBBI MANCINI, 1972; GIOBBI ORIGONI et al., 1982–83).

Mineral chemistry

Chemical analyses of minerals were performed using an ARL-SEMQ microprobe equipped with a Tracor-Northern energy dispersion solid-state detector. The system was operated at an accelerating voltage of 15 kV and a sample current on brass of 15 nA. The diameter of the beam was about 0.005 mm. Calibration was against natural standard minerals. The standards used for amphibole, garnet and plagioclase were kaersutite (Si, Al, Fe, Mg, Ca, Ti, Na, K) and rhodonite (Mn). The standards used for pyroxenes and spinels were kaersutite (Si, Al, Fe, Mg, Ca, Ti, Na, K), niccolite (Ni) and chromite (Cr), while the standards used for olivines were natural olivine (Si, Al, Fe, Mg, Ca, Ti, Na, K), niccolite (Ni) and chromite (Cr). The results were corrected for matrix effects using a modified version of the MAGIC IV program.

OLIVINE

The olivine of sample ML5s peridotite has a fairly homogeneous composition: Fo is around 86 mol%. NiO is between 0.09 and 0.12 wt% and MnO is between 0.18 and 0.24 wt%. In pyroxenites the Fo content of olivine ranges between 76 and 79 mol% (Tab. 4).

PYROXENES

Selected analyses on pyroxenes of Strona Ceneri Border Zone rocks are shown in tables 5 and 6.

Clinopyroxene. The clinopyroxenes of Mg# < 88 peridotite (ML5s) plot in the diopside field of the pyroxene quadrilateral (MORIMOTO et al., 1988) with composition $En_{50}Fs_2Wo_{48}$. Those of the pyroxenites have a mean composition of $En_{49}Fs_4$ Wo_{47}. In the garnet pyroxenite dyke the small grains of clinopyroxene that surround amphibole, have composition of $En_{45}Fs_4Wo_{51}$.

In the peridotite the Mg# of clinopyroxene has a mean value of 96, in the pyroxenites it varies from 89 to 97; in the intergranular clinopyroxene Mg# is 87. In the garnet pyroxenite dyke Mg# is 91–95.

In the amphibolites with garnet relics, the pyroxene in the symplectitic intergrowths is $En_{39}Fs_{11}Wo_{50}$.

Orthopyroxene. In peridotite no reliable data were obtained on the scarce and highly altered orthopyroxene relics. In pyroxenites, the orthopyroxenes plot in the field of enstatite: those enclosed in clinopyroxenes have a slightly lower En content than the rare intergranular grains.

SPINEL

Spinels are Cr-rich in the peridotites and Al-rich in the pyroxenites (Tab. 7 and Fig. 6a). In both rock types, spinels are characterized by low TiO_2 contents (up to 0.11 wt%).

In the peridotite the Mg# ranges between 54 and 61, with an average value of 57; Cr# [$Cr\# = 100 \cdot Cr/(Cr + Al)$] ranges between 23 and 28. The

Tab. 5 Selected microprobe analyses of clinopyroxene of Strona Ceneri Border Zone.

Rock type	Peridotite	Pyroxenites					Pyroxenite dyke	Amphibolites with garnet relicts		
Sample	ML5s	LUCR40 p4f6	LUCR40 p1f3	LUCR4B p2f16	LUCR4B intergran.	LDSC49 b3	ML2	MCMA40	MCMA52	MCMA55
SiO_2	53.57	51.09	49.56	50.85	51.12	51.59	54.48	51.42	52.31	52.63
TiO_2	0.19	0.54	0.71	0.75	0.53	0.51	0.17	0.04	0.02	0.05
Cr_2O_3	0.23	0.23	0.30	0.58	0.31	0.20	0.00	0.00	0.00	0.00
Al_2O_3	1.12	4.13	5.21	5.86	4.70	3.95	2.42	1.03	1.13	0.94
FeO	2.15	4.24	4.07	3.73	6.08	4.20	2.71	8.90	9.30	7.87
MnO	0.09	0.18	0.16	0.12	0.17	0.00	0.04	0.14	0.15	0.13
MgO	18.63	15.57	15.22	15.12	17.54	15.95	15.54	13.14	12.77	13.66
CaO	24.50	23.67	23.82	22.51	18.59	23.44	24.61	23.83	24.03	24.30
Na_2O	0.05	0.53	0.61	0.49	0.53	0.43	0.25	0.43	0.48	0.36
Tot.	100.53	100.18	99.66	100.01	99.57	100.27	100.22	98.93	100.19	99.94
Si	1.941	1.877	1.835	1.858	1.876	1.888	1.974	1.955	1.964	1.968
Ti	0.005	0.015	0.021	0.021	0.015	0.014	0.005	0.001	0.001	0.001
Cr	0.007	0.007	0.170	0.016	0.009	0.006	0.000	0.000	0.000	0.000
$Al^{(IV)}$	0.048	0.123	0.166	0.142	0.124	0.113	0.026	0.045	0.036	0.032
$Al^{(VI)}$	0.000	0.056	0.062	0.110	0.079	0.058	0.078	0.001	0.014	0.010
Fe^{3+}	0.034	0.069	0.099	0.009	0.045	0.051	0.000	0.073	0.056	0.045
Fe^{2+}	0.031	0.061	0.027	0.105	0.142	0.077	0.082	0.210	0.236	0.201
Mn	0.003	0.006	0.005	0.004	0.005	0.000	0.001	0.005	0.005	0.004
Mg	1.006	0.853	0.840	0.823	0.959	0.870	0.839	0.745	0.715	0.761
Ca	0.951	0.932	0.945	0.881	0.731	0.919	0.956	0.971	0.967	0.974
Na	0.004	0.038	0.044	0.035	0.038	0.031	0.018	0.032	0.035	0.026
Diopside	0.88	0.76	0.77	0.67	0.54	0.75	0.85	0.72	0.70	0.74
Wollastonite	0.47	0.41	0.40	0.38	0.31	0.41	0.47	0.46	0.47	0.47
Enstatite	0.50	0.43	0.42	0.41	0.48	0.44	0.42	0.37	0.36	0.38
Ferrosilite	0.02	0.03	0.01	0.05	0.07	0.04	0.04	0.11	0.12	0.10
Pyroxmangite	0.00	0.00	0.00	0.00	0.00	0.00	0.00	0.00	0.00	0.00
$CaAl_2SiO_6$	0.00	0.06	0.06	0.08	0.08	0.06	0.02	0.00	0.01	0.01
$CaFe_2SiO_6$	0.03	0.03	0.06	0.00	0.01	0.02	0.00	0.04	0.02	0.02
$CaCr_2SiO_6$	0.01	0.01	0.01	0.02	0.01	0.01	0.00	0.00	0.00	0.00
Acmite	0.00	0.04	0.04	0.01	0.04	0.03	0.00	0.03	0.04	0.03
Jadeite	0.00	0.00	0.00	0.03	0.00	0.00	0.02	0.00	0.00	0.00
$CaTiAl_2O_6$	0.01	0.02	0.02	0.02	0.02	0.01	0.01	0.00	0.00	0.00

The analyses of clinopyroxene of mafic rocks are averages of a large number of data in each sample. Structural formulae are normalized as suggested by LINDSLEY (1983).
The analyses of clino- and orthopyroxenes that are in mutual contact bear the same labels (e.g., p4f6 of sample LUCR40). LUCR4B clinopyroxene labelled as intergranular is a small grain at the border of the p2f16 clinopyroxene.

Cr content of the intergranular spinels present at the olivine grain boundaries is higher relative to that of the spinel-exolutions in clinopyroxene. A slight chemical zoning can be detected in the large intergranular spinels: Al_2O_3 and MgO decrease from core to rim, while Cr_2O_3 and FeO increase.

In the pyroxenites, cumulus spinels exhibit a range in Cr# from 5 to 18. Mg# ranges from 37 to 55, with an average of 45.

In figure 7b spinels from the Strona Ceneri Border Zone are compared with those of the Balmuccia peridotitic body in the Ivrea Verbano Zone (GARUTI et al., 1980). The peridotite spinels plot in the field of the rims of the spinels of the Ivrea Verbano Zone mantle peridotite. Those of the pyroxenite plot on a parallel trend below that of the Ivrea Verbano Zone cumulitic peridotites.

In the pyroxenite spinels the TiO_2 content is correlated positively with Cr#, and negatively with the Fo content of the coexisting olivine, i.e. spinel generally becomes richer in Ti and Cr as olivine becomes richer in Fe, suggesting an increase in activity of Si, Fe and Ti in the magmatic liquid due to early fractionation of a large amount

Tab. 6 Selected microprobe analyses of orthopyroxene of pyroxenites from Strona Ceneri Border Zone.

Rock type	Pyroxenites						
Sample	LUCR40 p4f6	LUCR40 p1f3	LUCR40 p1f0	LUCR4B p2f16	LUCR4B p3f23	LDSC49 a7	LDSC49 b3
SiO_2	52.89	52.72	51.02	52.23	51.36	52.81	53.38
TiO_2	0.12	0.08	0.17	0.11	0.16	0.07	0.06
Cr_2O_3	0.14	0.17	0.25	0.21	0.33	0.17	0.14
Al_2O_3	3.94	3.05	5.40	4.22	4.70	3.98	4.01
FeO	13.09	13.06	13.60	11.92	12.15	14.72	14.17
MnO	0.33	0.28	0.29	0.27	0.28	0.00	0.00
MgO	28.87	29.90	27.76	29.77	28.98	27.91	28.78
CaO	0.67	0.24	0.48	0.59	0.49	0.23	0.22
Na_2O	0.00	0.00	0.00	0.00	0.00	0.00	0.00
Tot.	100.05	99.50	98.97	99.32	98.45	99.89	100.76
Si	1.888	1.893	1.848	1.871	1.859	1.896	1.894
Ti	0.003	0.002	0.005	0.003	0.004	0.002	0.002
Cr	0.004	0.005	0.007	0.006	0.009	0.005	0.004
$Al^{(IV)}$	0.112	0.107	0.152	0.130	0.141	0.104	0.106
$Al^{(VI)}$	0.054	0.022	0.079	0.049	0.059	0.064	0.061
Fe^{3+}	0.000	0.064	0.042	0.074	0.063	0.073	0.038
Fe^{2+}	0.391	0.328	0.371	0.283	0.305	0.369	0.383
Mn	0.010	0.009	0.009	0.008	0.009	0.000	0.000
Mg	1.536	1.600	1.499	1.589	1.563	1.494	1.522
Ca	0.026	0.009	0.019	0.023	0.019	0.009	0.008
Na	0.000	0.000	0.000	0.000	0.000	0.000	0.000
Diopside	0.02	0.01	0.02	0.02	0.02	0.01	0.01
Wollastonite	0.01	0.01	0.01	0.01	0.01	0.00	0.00
Enstatite	0.74	0.76	0.70	0.74	0.73	0.71	0.72
Ferrosilite	0.19	0.16	0.17	0.13	0.14	0.17	0.18
Pyroxmangite	0.01	0.00	0.00	0.00	0.00	0.00	0.00
$R^2R^3AlSiO_6$	0.06	0.09	0.13	0.12	0.13	0.10	0.10
$NaR^3Si_2O_6$	0.00	0.00	0.00	0.00	0.00	0.00	0.00
$NaTiAlSiO_6$	0.00	0.00	0.00	0.00	0.00	0.00	0.00
$R^2TiAlSiO_6$	0.00	0.00	0.01	0.00	0.00	0.00	0.00

Structural formulae are normalized as suggested by LINDSLEY (1983); the end-member of each sample is also shown. The label p1f0 indicates a grain of orthopyroxene enclosed in the p4f6 clinopyroxene and the label a7 an orthopyroxene enclosed in the b3 clinopyroxene.

of magnesian olivine (ALLAN et al., 1988; BALLANTYNE, 1992).

AMPHIBOLE

All analysed amphiboles (Tab. 8) show an irregular compositional variability. According to the classification of LEAKE (1978) they are mainly Mg-hornblendes. In some pyroxenites and metagabbros they are tschermakitic hornblendes or tschermakites. In amphibolites with garnet relics, showing a retrograde overprint, some actinolitic hornblendes have also been detected.

The amphibole that grows at the boundary between clinopyroxene and olivine is pargasitic hornblende with an average $Mg/(Mg + Fe^{2+})$ of about 0.88 in pyroxenite and 0.96 in peridotite. An average $Mg/(Mg + Fe^{2+})$ of 0.97 is characteristic for the amphiboles of the pyroxenite dyke.

In the cumulitic metagabbros the amphibole $Mg/(Mg + Fe^{2+})$ varies between 0.74 and 0.93. In the amphibolites with garnet relics the range is 0.53–0.79. In the small amphibolite boudins enclosed in the serpentinized peridotite of Alpe di Zalto (samples ML7 and LRSC35), the amphibole $Mg/(Mg + Fe^2)$ value is 0.88.

GARNET

Garnet has been analyzed in a sample of pyroxenite dyke and in 11 samples of amphibolites;

Tab. 7 Selected microprobe analyses of spinel of ultramafites of Strona Ceneri Border Zone.

Rock type	Peridotite		Pyroxenite	
Sample	ML5s-1	ML5s-2	LDSC49-3	LDSC49-4
SiO_2	0.03	0.33	0.00	0.95
TiO_2	0.07	0.09	0.08	0.05
Cr_2O_3	20.24	22.16	14.18	10.93
Al_2O_3	45.28	40.74	46.88	51.91
Fe_2O_3	3.71	6.20	4.44	0.71
FeO	18.65	16.46	26.04	24.73
MnO	0.12	0.26	0.23	0.00
MgO	13.62	14.27	8.65	10.97
NiO	0.08	0.00	0.08	0.09
CaO	0.00	0.18	0.00	0.00
Na_2O	0.03	0.06	0.02	0.01
K_2O	0.01	0.05	0.00	0.00
Tot.	101.84	100.79	100.59	100.35
Si	0.001	0.009	0.000	0.026
Ti	0.002	0.002	0.002	0.001
Cr	0.443	0.495	0.321	0.239
Al	1.477	1.356	1.581	1.692
Fe^{3+}	0.077	0.132	0.096	0.015
Fe^{2+}	0.432	0.389	0.623	0.572
Mn	0.003	0.006	0.006	0.000
Mg	0.562	0.601	0.369	0.452
Ni	0.002	0.000	0.002	0.002
Ca	0.000	0.005	0.000	0.000
Na	0.002	0.003	0.001	0.001
K	0.000	0.002	0.000	0.000
Mag	0.02	0.03	0.03	0.00
Mg-Ferrite	0.02	0.04	0.02	0.00
Spl	0.42	0.41	0.29	0.38
Hc	0.32	0.26	0.49	0.48
Chr	0.10	0.10	0.10	0.07
Mg-Chr	0.13	0.15	0.06	0.05
xMgSpl	0.56	0.60	0.37	0.44
$xFe^{2+}Spl$	0.43	0.39	0.62	0.56
yAlSpl	0.74	0.68	0.79	0.87
yCrSpl	0.22	0.25	0.16	0.12
$yFe^{3+}Spl$	0.04	0.07	0.05	0.01

ML5s-1 is an exsolved patch in clinopyroxene,
ML5s-2 is an intergranular brownish crystal;
LDSC49-3 and LDSC4 are the rim and the core of a greenish intergranular grain.
Structural formulae calculated on the basis of 3 cations.

Table 9 and figure 7a show the chemical composition of representative samples.

In the pyroxenite dyke (ML2) garnet is $Alm_{34-39}Prp_{28-35}Grs_{27-33}Sps_{2-3}$. A slight zoning has been observed from core to rim, with increasing MgO and decreasing CaO.

In the amphibolites, the chemical composition of garnets is usually homogeneous (112 analyses): $Alm_{46-59}Grs_{23-31}Prp_{9-14}Sps_{2-7}$. Exceptions are garnets of samples ML7 ($Alm_{58-37}Prp_{24-35}Grs_{17-25}$) and LRSC35 ($Alm_{46-35}Prp_{33-37}Grs_{16-26}$), which have a higher pyrope content similar to that of the pyroxenite dyke (ML2).

A slight zoning from core to rim has been observed in almost all the garnets of the amphibolites; the inset in figure 7a shows an example of the zoning for the sample LRSC33. In sample LRSC50, where there are both coarse- and fine-grained populations, the garnets show the same composition ($Alm_{54-60}Prp_{10-14}Grs_{20-27}$), except for the MnO content, that is around 0.35 wt% in the coarse grains, and around 3.35 in the small ones. MnO content is generally below 1.00 wt% in the other samples of amphibolites.

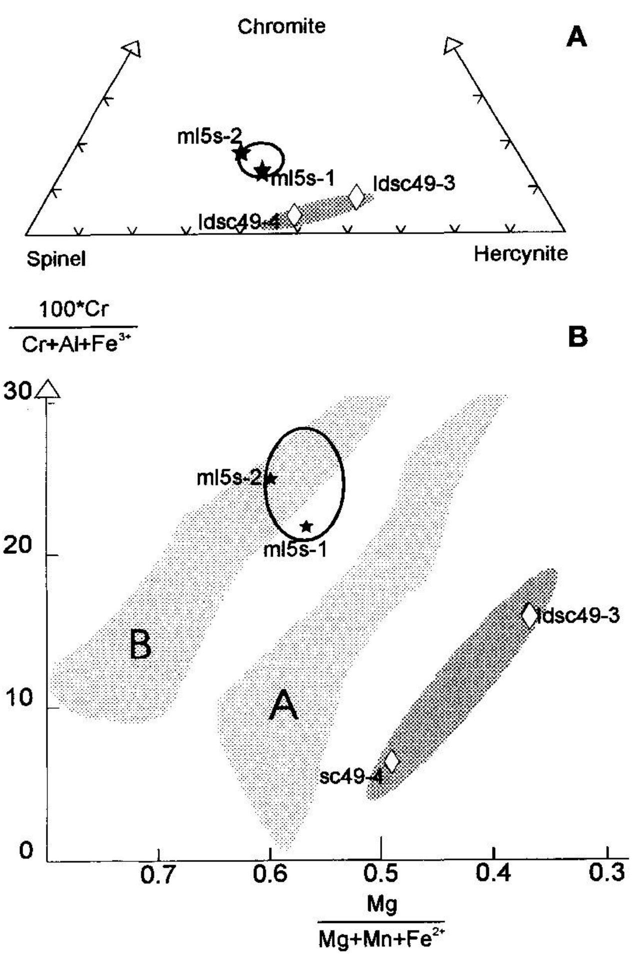

Fig. 6 (A) Classificatory diagram of spinel in ultramafic rocks. (B) Composition of spinel in terms of $Mg/(Mg+Fe^{2+}+Mn)$, and $Cr/(Cr+Al+Fe^{3+})$: Solid line: field of peridotite, dark shade area: pyroxenite; full star = peridotite; diamond = pyroxenite. Light shaded fields represent spinels in cumulitic peridotites (A) and mantle peridotites (B) from Balmuccia (Ivrea Verbano Zone, GARUTI et al., 1980, Fig. 6).

Tab. 8 Selected microprobe analyses of amphibole of ultramafites and metabasites of Strona Ceneri Border Zone.

Rock type	Peridotite		Pyroxenites				Pyroxenite dyke		Metagabbros			
Sample	ML5s		LUCR1		LUCR5b		ML2		LRSC44		ML4	
	X	s.d.	X	s.d.	X	s.d.	X	s.d.	X	s.d.	X	s.d.
SiO_2	49.04	*(1.89)*	46.83	*(1.65)*	46.42	*(1.39)*	47.40	*(1.98)*	47.69	*(1.63)*	45.84	*(1.17)*
TiO_2	0.46	*(0.12)*	0.33	*(0.08)*	0.32	*(0.13)*	0.68	*(0.21)*	0.27	*(0.05)*	0.23	*(0.07)*
Al_2O_3	11.48	*(1.73)*	11.44	*(1.42)*	10.87	*(1.74)*	12.80	*(1.91)*	12.61	*(1.95)*	16.08	*(1.11)*
FeO	4.22	*(0.32)*	6.75	*(0.53)*	8.68	*(0.42)*	7.05	*(0.62)*	8.50	*(0.34)*	7.38	*(0.43)*
MnO	0.08	*(0.02)*	0.14	*(0.04)*	0.19	*(0.03)*	0.11	*(0.04)*	0.16	*(0.05)*	0.13	*(0.03)*
MgO	19.77	*(0.74)*	17.26	*(0.87)*	16.04	*(0.76)*	17.60	*(1.04)*	15.55	*(0.75)*	15.13	*(0.66)*
CaO	13.26	*(0.41)*	12.34	*(0.20)*	12.26	*(0.09)*	12.40	*(0.76)*	12.14	*(0.23)*	11.64	*(0.07)*
Na_2O	1.97	*(0.38)*	1.96	*(0.23)*	1.50	*(0.27)*	1.87	*(0.44)*	1.48	*(0.23)*	1.86	*(0.08)*
K_2O	0.09	*(0.11)*	0.35	*(0.04)*	0.31	*(0.07)*	0.31	*(0.07)*	0.15	*(0.05)*	0.14	*(0.05)*
Tot	99.19		97.4		96.59		100.22		98.55		98.43	
Si	6.668		6.613		6.646		6.471		6.653		6.353	
$Al^{(IV)}$	1.358		1.387		1.354		1.529		1.347		1.647	
$Al^{(VI)}$	0.475		0.518		0.481		0.531		0.727		0.981	
Ti	0.469		0.035		0.034		0.069		0.029		0.024	
Fe^{2+}	0.070		0.332		0.469		0.124		0.487		0.220	
Fe^{3+}	0.408		0.465		0.570		0.681		0.505		0.635	
Mn	0.009		0.017		0.023		0.013		0.019		0.015	
Mg	3.991		3.633		3.422		3.581		3.233		3.125	
Ca	1.924		1.867		1.881		1.814		1.815		1.729	
Na	0.517		0.536		0.416		0.496		0.401		0.500	
K	0.016		0.063		0.057		0.054		0.027		0.025	
Mg#	0.98		0.92		0.88		0.97		0.87		0.93	

(to be continued)

PLAGIOCLASE

Plagioclase compositions (Tab. 10) of metagabbros and amphibolites with garnet relics are highly variable (An_{10} to An_{70}).

In the metagabbros the An content of the large zoned plagioclase grains is about 67% in the core and 62% in the rim, the An content of the recrystallized plagioclase of the polygonal aggregates is generally lower (45–54 An%) (Fig. 7b).

In amphibolites with garnet relics there is a significant difference between the plagioclase of the symplectite (An 10–29%) and that of the coronas (An 33–49%), even in the most recrystallized samples (Fig. 7b). The coronitic plagioclase show a slightly direct zoning from 38 An% to 33 An%.

Geothermobarometry

The WOOD and BANNO (1973) formulation for the temperature dependence of Mg/Fe distribution between coexisting ortho- and clinopyroxenes from pyroxenites LUCR40 and LUCR4b, gives a temperature estimate of 846–922 °C using core data. Lower temperatures (about 750 °C) have been obtained using rim data. A higher temperatures range of 930–1046 °C has been calculated on the same samples using opx enclosed in cpx. These temperature differences are also confirmed by the geothermometers of BREY and KÖHLER (1990) and WELLS (1977). It must be noted that these calibrations give temperature values that are 70–80 °C lower than those obtained with the geothermometer of Wood and Banno. Using the method proposed by GASPARIK (1984) on a sample of pyroxenite with Cpx and Opx coexisting with Ol and Spl, a rough estimate of a P = 12 kb has been obtained. These T-P estimates suggest high amphibolite-granulite facies conditions.

The geothermometer based on the content of Ca in plagioclase and Al in coexisting amphibole (PLYUSNINA, 1982) and the other one based on the content of Ti in amphiboles crystallised at T < 970 °C (OTTEN, 1984), suggest temperatures in the range of 590–690 °C for amphiboles from amphibolites, a range of 570–590 °C for amphiboles from metagabbros, and a range of 577–612 °C for the intergranular amphiboles from ultramafic rocks. A P of about 6–8 kb can also be inferred (PLYUSNINA, 1982).

Tab. 8 continued

Rock type	Amphibolites with garnet relics													
Sample	LRSC33		LRSC35		ML7		MCMA26		MCMA55		LRSC50		LRSC50 kel.-2	LRSC50 sym.-2
	X	s.d.	X	s.d.	X	s.d.	X	s.d.	X	s.d.	X	s.d.		
SiO_2	47.42	*(2.17)*	46.08	*(1.83)*	45.23	*(1.20)*	43.61	*(1.94)*	44.52	*(2.04)*	46.44	*(1.97)*	46.94	45.38
TiO_2	0.80	*(0.22)*	0.65	*(0.18)*	0.71	*(0.35)*	0.77	*(0.17)*	0.60	*(0.23)*	0.49	*(0.11)*	0.60	0.56
Al_2O_3	8.21	*(1.83)*	13.67	*(1.63)*	14.48	*(1.35)*	11.49	*(2.23)*	10.74	*(2.44)*	12.16	*(2.06)*	11.62	14.07
FeO	19.02	*(1.19)*	11.56	*(0.98)*	11.79	*(0.57)*	17.42	*(0.60)*	16.81	*(1.65)*	13.25	*(1.18)*	13.67	12.41
MnO	0.15	*(0.03)*	0.15	*(0.04)*	0.15	*(0.04)*	0.22	*(0.03)*	0.22	*(0.04)*	0.18	*(0.04)*	0.28	0.18
MgO	11.00	*(1.62)*	13.61	*(0.89)*	13.22	*(0.71)*	9.42	*(1.02)*	9.84	*(1.46)*	13.03	*(1.36)*	12.48	12.77
CaO	10.34	*(0.89)*	11.05	*(0.62)*	10.98	*(0.30)*	12.12	*(0.18)*	12.22	*(0.23)*	11.41	*(0.43)*	11.40	11.58
Na_2O	1.47	*(0.42)*	1.30	*(0.25)*	1.48	*(0.25)*	1.19	*(0.25)*	1.15	*(0.28)*	1.43	*(0.22)*	1.46	1.65
K_2O	0.19	*(0.04)*	0.26	*(0.09)*	0.18	*(0.04)*	0.57	*(0.13)*	0.61	*(0.19)*	0.21	*(0.11)*	0.13	0.17
Tot	98.60		98.33		98.22		96.81		96.71		98.60		98.58	98.77
Si	6.840		6.458		6.355		6.552		6.688		6.577		6.749	6.416
$Al^{(IV)}$	1.160		1.542		1.645		1.448		1.312		1.423		1.320	1.584
$Al^{(VI)}$	0.236		0.717		0.753		0.587		0.590		0.607		0.628	0.761
Ti	0.087		0.069		0.075		0.087		0.068		0.052		0.064	0.060
Fe^{2+}	1.186		0.385		0.386		1.861		1.912		0.751		0.966	0.754
Fe^{3+}	1.108		0.970		1.000		0.327		0.201		0.818		0.661	0.713
Mn	0.018		0.018		0.018		0.028		0.028		0.021		0.034	0.022
Mg	2.365		2.842		2.768		2.109		2.202		2.750		2.647	2.691
Ca	1.598		1.659		1.653		1.951		1.967		1.732		1.738	1.754
Na	0.411		0.354		0.404		0.347		0.336		0.393		0.403	0.452
K	0.035		0.047		0.032		0.110		0.117		0.037		0.024	0.031
Mg#	0.67		0.88		0.88		0.53		0.54		0.79		0.62	0.65

X = average; s.d. standard deviation; sym. = symplectitic; kel. = kelyphitic
Structural formulae calculated on the basis of 13 cations = Si + Ti + Al + Fe + Mn + Mg, as suggested by COSCA et al. (1991).

Concluding remarks

The Strona Ceneri Border Zone mainly consists of banded amphibolites probably derived from basaltic tuffites finely interlayered with siliciclastic sediments. In some places along the horizon, the banded amphibolites contain lenses of more or less serpentinized mantle peridotite with websterite veins, pyroxenite, metagabbro and massive amphibolite with garnet relics. These amphibolites show a MORB geochemical signature; they represent more or less fractionated liquids that seem to bear no relationships with the associated mantle peridotites.

The metamorphic peridotites represent a fertile mantle not depleted in Sc and LREE. They still carry relics of the mantle minerals, i.e. orthopyroxene, olivine, and spinel which indicate their derivation from a spinel lherzolite mantle. Their association with MOR metabasalts, metagabbro and pyroxenite may reflect a situation of some modern oceanic rifts in which unroofing of subcontinental mantle was followed by extrusion of basalts and formation of an oceanic crust (PICCARDO et al., 1992).

Their crustal history is documented by deformation, replacement of spinel by clinochlore, exsolution of secondary green spinel lamellae in the pyroxene and growth of pargasitic amphibole and serpentine minerals.

The pyroxenites have REE depleted patterns which are characteristic of rocks crystallized from a tholeiitic melt. Their granoblastic texture suggest recrystallization in metamorphic conditions: a temperature of equilibration higher than 800 °C and a P of about 12 kb have been estimated. These P and T estimates suggest a lower crustal environment. Such conditions might be responsible for the formation in the metabasites of the garnet. Even higher pressure conditions are suggested by the presence, in some amphibolites, of Amph-Pl kelyphite around garnet and Di (Amph)-Pl symplectite, that probably represent the products of transformation of an eclogitic assemblage. In the studied samples no omphacite relics have been found so far. However the microcrystalline sym-

Tab. 9 Selected microprobe analyses of garnet of Strona Ceneri Border Zone

Rock type	Pyroxenite dyke	Amphibolites with garnet relics										
Sample	ML2	LRSC33	LRSC35	LRSC39	LRSC40	LRSC50	ML7	MCMA26	MCMA40	MCMA51	MCMA52	MCMA55
SiO_2	39.53	38.75	39.95	37.66	37.87	39.36	38.38	37.59	37.73	37.55	37.69	37.44
TiO_2	0.08	0.06	0.12	0.09	0.06	0.12	0.17	0.21	0.24	0.14	0.16	0.16
Al_2O_3	21.71	21.40	22.50	23.26	22.87	21.60	22.66	21.06	21.54	21.15	21.04	21.17
FeO	18.98	27.00	19.24	26.42	27.46	27.32	19.32	22.68	26.31	25.10	25.13	25.86
MnO	1.22	0.64	0.14	0.46	1.10	0.38	0.36	3.09	1.76	2.76	1.61	0.93
MgO	7.78	4.19	9.23	2.53	4.44	3.50	8.31	2.28	2.23	3.55	2.71	3.00
CaO	11.17	8.92	10.12	11.41	6.46	9.60	10.16	13.16	10.38	8.71	11.26	10.78
Na_2O	0.00	0.04	0.02	0.01	0.01	0.03	0.00	0.00	0.00	0.00	0.00	0.00
Tot.	100.47	101.00	101.32	101.84	100.27	101.91	99.36	100.07	100.19	98.96	99.60	99.34
Si	2.993	3.009	2.976	2.907	2.961	3.038	2.926	2.958	2.982	2.988	2.983	2.967
Ti	0.005	0.004	0.007	0.005	0.004	0.007	0.010	0.012	0.014	0.008	0.010	0.010
$Al^{(IV)}$	0.007	0.000	0.024	0.093	0.039	0.000	0.074	0.042	0.018	0.012	0.017	0.033
$Al^{(VI)}$	1.931	1.959	1.951	2.023	2.068	1.965	1.961	1.912	1.988	1.972	1.945	1.944
Fe^{3+}	0.067	0.022	0.063	0.061	0.000	0.000	0.092	0.105	0.002	0.024	0.053	0.069
Fe^{2+}	1.135	1.731	1.135	1.644	1.795	1.763	1.138	1.388	1.737	1.647	1.610	1.645
Mn	0.078	0.042	0.009	0.030	0.073	0.025	0.023	0.206	0.118	0.186	0.108	0.062
Mg	0.878	0.485	1.025	0.291	0.517	0.403	0.944	0.268	0.263	0.421	0.320	0.354
Ca	0.906	0.742	0.808	0.944	0.541	0.794	0.830	1.110	0.879	0.743	0.955	0.915
Alm	0.38	0.58	0.38	0.57	0.61	0.59	0.39	0.47	0.58	0.55	0.54	0.55
Grs	0.27	0.23	0.24	0.29	0.18	0.26	0.23	0.31	0.29	0.23	0.29	0.27
Prp	0.29	0.16	0.34	0.10	0.18	0.14	0.32	0.09	0.09	0.14	0.11	0.12
Sps	0.03	0.01	0.00	0.01	0.03	0.01	0.01	0.07	0.04	0.06	0.04	0.02
Anr	0.03	0.01	0.03	0.03	0.00	0.00	0.05	0.05	0.00	0.01	0.03	0.04

Structural formulae calculated on the basis of 7 cations.

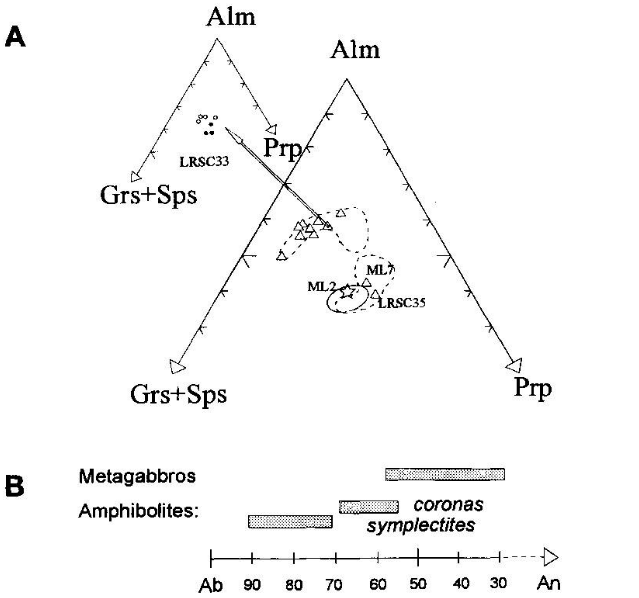

Fig. 7 (A) Compositional variation of garnets in the (Grs + Sps)-Alm-Prp diagram. Triangles: selected samples of amphibolites with garnet relics. Open star = garnet pyroxenite dyke. Dotted line: field of garnets of amphibolites with garnet relics. Solid line: field of garnets of the garnet pyroxenite dyke. The inset shows an example of compositional variation from core (full circles) to rim (open circles) in a garnet of an amphibolite (LRSC33). (B) An% variation of plagioclases in selected samples of amphibolites with garnet relics and metagabbros.

plectites, the compositional differences between the plagioclase of coronas and that of the symplectites, as well as the occurrence of rutile with rims of ilmenite and sphene, suggest an earlier high pressure event for these rocks.

The replacement of pyroxene (omphacite?) by amphibole-plagioclase symplectite and the garnet destabilization may have started during a pre- or early Variscan post-subduction event and continued during the main Variscan metamorphism. The textural relationships do not give unequivocal indication about the timing of this process.

The described features are common in amphibolites of various age and provenance, e.g. in the Rhodope Zone – NNE Greece and Bulgaria (LIATI and MPOSKOS, 1990), in the Black Forest of Germany (KLEIN and WIMMENAUER, 1984), in the Bohemian Massif (MESSIGA and BETTINI, 1990), in the Massif Central of France (SANTALLIER, 1983), in the Western Alps (LIÉGEOIS and DUCHESNE, 1981; DAL PIAZ et al., 1993; CAPELLI et al., 1994), in the Central Alps (HEINRICH, 1983, BIINO, 1995). In many cases it is possible to observe all transformation stages of eclogite to amphibolite. The original omphacite is transformed into a symplectite of Ca-rich clinopyroxene and plagioclase,

Tab. 10 Selected microprobe analyses of plagioclase of metabasites of Strona Ceneri Border Zone

Rock type	Metagabbros		Amphibolites with garnet relics								
Sample	LRSC44	ML4 core	LRSC35 sympl.	LRSC35 coron.	LRSC39 sympl.	LRSC40 sympl.	LRSC40 coron.	LRSC50 sympl.	LRSC50 coron.	ML7 sympl.	ML7 coron.
SiO_2	56.36	50.91	60.20	56.39	66.27	62.17	58.32	62.15	58.94	60.42	58.20
TiO_2	0.02	0.00	0.00	0.00	0.01	0.04	1.85	0.00	0.00	0.00	0.00
Al_2O_3	27.96	31.31	25.95	27.72	21.08	24.96	24.39	23.31	25.92	25.14	26.80
FeO	0.00	0.02	0.00	0.26	0.21	0.26	0.98	0.16	0.38	0.36	0.26
MnO	0.00	0.05	0.02	0.05	0.00	0.01	0.01	0.00	0.02	0.00	0.00
MgO	0.00	0.00	0.01	0.00	0.14	0.04	0.09	0.02	0.04	0.02	0.00
CaO	9.93	14.15	5.63	9.42	2.01	5.71	7.31	5.20	7.39	5.46	7.69
Na_2O	6.33	3.60	8.74	6.45	10.35	7.73	7.14	9.07	7.28	8.56	7.35
K_2O	0.15	0.01	0.01	0.02	0.00	0.07	0.50	0.08	0.22	0.08	0.07
Tot	100.75	100.05	100.56	100.31	100.07	100.99	100.59	99.99	100.19	100.04	100.37
Si	2.506	2.314	2.645	2.519	2.914	2.749	2.610	2.749	2.627	2.676	2.585
Ti	0.001	0.000	0.000	0.000	0.000	0.001	0.062	0.000	0.000	0.000	0.000
Al	1.466	1.677	1.344	1.459	1.092	1.301	1.286	1.228	1.362	1.312	1.403
Fe^{3+}	0.000	0.001	0.000	0.010	0.000	0.000	0.018	0.007	0.013	0.012	0.010
Fe^{2+}	0.000	0.000	0.000	0.000	0.008	0.010	0.019	0.000	0.000	0.000	0.000
Mn	0.000	0.002	0.001	0.002	0.000	0.000	0.000	0.000	0.001	0.000	0.000
Mg	0.000	0.000	0.001	0.000	0.009	0.003	0.006	0.003	0.003	0.001	0.000
Ca	0.473	0.689	0.265	0.451	0.095	0.271	0.351	0.246	0.353	0.259	0.366
Na	0.546	0.317	0.745	0.559	0.882	0.663	0.620	0.778	0.629	0.735	0.633
K	0.009	0.001	0.001	0.001	0.000	0.004	0.029	0.005	0.013	0.005	0.004
Ab	0.53	0.32	0.74	0.55	0.90	0.71	0.62	0.76	0.63	0.74	0.63
An	0.46	0.68	0.26	0.45	0.10	0.29	0.35	0.24	0.36	0.26	0.37
Or	0.01	0.00	0.00	0.00	0.00	0.00	0.03	0.00	0.01	0.00	0.00

sympl. = symplectitic, coron. = coronitic.
The formulae are normalized on the basis of 5 cations.

while garnet is surrounded by kelyphite consisting of diopside and plagioclase. Subsequently the Ca-pyroxene of the symplectites is completely replaced by amphibole. These particular textures are commonly attributed to a post-eclogitic retrogression due to both pressure release during exhumation, and to a temperature increase during the thermal relaxation following collision and subduction.

In the case of Serie dei Laghi the amphibolite facies overprint is very strong and could have obliterated almost all the previous textures. A rough estimate of T and P conditions of this overprint on the amphibolites, yields about 600 °C and 6–8 kb.

From the geological point of view, these rocks, according to the chronological and paleogeographical scheme proposed by MATTE (1991), may be regarded as Variscan ophiolites. According to this author, the Austroalpine nappes, and consequently the Southalpine basement, mostly correspond to the internal part of the Variscan belt (VON RAUMER, 1984) deeply eroded before the Westphalian.

The Strona Ceneri Border Zone rocks could therefore belong to the southern suture, which is characterized by the occurrence of mafic-ultramafic rocks (metabasalts, metagabbros and serpentinites), with remnants of high pressure rocks. The age of the high pressure event is not well constrained. In our case it must predate the intrusion of the Ordovician granites (about 460 Ma), where they are often found as xenoliths. In Southern Brittany the age of the HP event is estimated between 420 and 360 Ma (PEUCAT, 1986; PAQUETTE, 1987). Eclogites of the Münchberg Klippe (Bavaria) are dated around 500 Ma by GEBAUER and GRÜNENFELDER (1979); the eclogitic event in the central and western Ötztal basement is 350–360 Ma (MILLER and THÖNI, 1995).

As regards the metamorphic history of the the Strona Ceneri Border Zone rocks, it appears that only some of the lithotypes underwent a HP event predating the main Variscan metamorphism and therefore the rocks with HP relics (i.e. amphibolites with garnet relics) were incorporated as clasts in the sedimentary protolith of this sequence.

Acknowledgements

This work was supported by the 60% MURST and by the 40% MURST grants "Basamenti cristallini e granitoidi circum-mediterranei: implicazioni geodinamiche" to A. Boriani and by 40% MURST and CNR grants to L. Morten. Microprobe facilities were supplied by Centro di Studio per la Geodinamica Alpina e Quaternaria-CNR, Milano.

References

ALLAN, J. F., SACK, R.O. and BATIZA R. (1988): Cr rich spinels as petrogenetic indicators: MORB-type lavas from the Lamont seamount chain, eastern Pacific. Amer. Mineral., 73, 741–753.

BALLANTYNE, P. (1992): Petrology and geochemistry of the plutonic rocks of the Halmahera ophiolite, eastern Indonesia, an analogue of modern oceanic forearcs. In: PARSON, M. L., MURTON, B.J. and BROWNING P. (eds): Ophiolites and their modern oceanic analogues, Geol. Soc. Special Publication No 60, 179–202.

BEDINI, R.M. (1995): Studio geochimico-petrologico degli xenoliti ultrafemici di Mega (Sidamo, Ethiopia-rift Africano Orientale): implicazioni sui processi di interazione magma-roccia nel mantello litosferico subcontinentale. Ph. D. Thesis, Università di Bologna.

BIINO, G. (1995): Pre-Variscan evolution of the eclogitised mafic rocks from the Helvetic basement of the Central Alps. Eur. J. Mineral., 7, 57–70.

BORIANI, A. and GIOBBI MANCINI, E. (1972): The feldspathized amphibolites of the Strona Ceneri Zone. Boll. Soc. Geol. Ital., 91, 655–681.

BORIANI, A., BURLINI, L. and SACCHI, R. (1990a): The Cossato-Mergozzo-Brissago line and the Pogallo line (Southern Alps, N-Italy) and their relationships with the late-Hercynian magmatic and metamorphic events. Tectonophysics, 182, 91–102.

BORIANI, A., GIOBBI ORIGONI, E., BORGHI, A. and CAIRONI, V. (1990b): The evolution of "Serie dei Laghi" (Strona Ceneri and Scisti dei Laghi), Southern Alps, N-Italy and Ticino, Switzerland. Tectonophysics, 182, 103–118.

BORIANI, A., GIOBBI ORIGONI, E. and PINARELLI, L. (1995): Paleozoic evolution of southern Alpine crust (northern Italy) as indicated by contrasting granitoid suites. Lithos, 35, 47–63.

BOUCHARDON, J.P, SANTALLIER, D., BRIAND, B., MENOT, R.P. and PIBOULE, M. (1989): Eclogites in the French paleozoic orogen: geodynamic significance. Tectonophysics, 169, 317–322.

BREY, G.P. and KÖHLER, T. (1990): Geothermobarometry in four-phase Lhezolites II. New thermobarometers, and practical assessment of existing thermobarometers. J. Petrol., 31, 353–378.

CAPELLI, C., CORTESOGNO, L. and GAGGERO, L. (1994): Metabasites and associated ultramafites in the crystalline basement of Ligurian Alps: petrochemical characterisation, geotectonic significance. Per. Mineral., 63, 179–197.

COSCA, M.A., ESSENE, E.J. and BROWN, J.R. (1991): Complete chemical analysis of metamorphic hornblendes: implications for normalizations, calculated H_2O activities, and thermobarometry. Contrib. Mineral. Petrol., 108, 472–484.

DAL PIAZ, G.V., GOSSO, G., PENNACCHIONI, G. and SPALLA, M.I. (1993): Geology of eclogites and related rocks in the Alps. In: MORTEN, L. (ed.): Italian eclogites and related rocks, Acc. Naz. Sci. Scritti e doc. XIII, 17–58.

DOWNES, H., BODINIER, J.L., DUPUY, C., LEYEROUP, A. and DOSTAL, J. (1989): Isotope and trace-element heterogeneities in high-grade basic metamorphic rocks of Marvejols: tectonic implications for the Hercynian suture zone of the French Massif Central. Lithos, 24, 37–54.

FORESTIER, F.H. (1963): Métamorphisme hercynien dans les bassins du Haut Allier. Bull. Serv. Carte Géol. France, 271, 294 pp.

GARUTI, G., RIVALENTI, G., ROSSI, A., SIENA, F. and SINIGOI, S. (1980): The Ivrea Verbano mafic ultramafic complex of the Italian Western Alps: discussion of some petrological problems and a summary. Rend. Soc. It. Min. Petrol., 36 (2): 717–749.

GASPARIK, T. (1984): Two-pyroxene thermobarometry with new experimental data in the system CaO–MgO–Al_2O_3–SiO_2. Contrib. Mineral. Petrol., 87, 87–97.

GEBAUER, D. and GRÜNENFELDER, M. (1979): U/Pb zircon, Rb/Sr mineral dating of eclogites and their country rocks. Example: Münchberg Gneiss Massif, Northeast Bavaria. Earth Planet. Sci. Lett., 42, 35–44.

GIOBBI ORIGONI, E., TESTA, B. and CARIMATI, R. (1982–83): Contributo alla ricostruzione stratigrafica della "Serie dei Laghi": litofacies principali della "Strona-Ceneri" a NE del Lago Maggiore (Alpi Meridionali – Italia): Rend. Soc. It. Min. Petrol., 38, 1337–1350.

GRAETER, P. (1951): Geologie und Petrographie des Malcantone (südliches Tessin): Schweiz. Mineral. Petrogr. Mitt., 31, 361–483.

HEINRICH, C.A. (1983): Die regionale Hochdruckmetamorphose der Adula-Decke, Zentralalpen (Schweiz): Thesis, 7282, E.T.H. Zürich.

JAGOUTZ, E., PALME, H., BADDENHAUSEN, H., BLUM, K., CENFALES, M., DREIBUS, G., SPETTEL, B., LORENZ, V. and WAENKE, H. (1979): The abundances of major, minor, trace elements in the earth mantle as derived from primitive ultramafic nodules. Proc. Lunar. Planet. Sci. Conf. 10th, 2031–2050.

KAY, R., HUBBARD, N.J. and GAST, P.W. (1970): Chemical characteristics and origin of oceanic ridge volcanic rocks. J. Geophys. Res., 75, 1585–1613.

KELTERBORN, P. (1923): Geologische und petrographische Untersuchungen im Malcantone. Verh. Nat. Ges. Basel, 34, 128–232.

KLEIN, H. and WIMMENAUER, W. (1984): Eclogites and their retrograde transformation in the Schwarzwald (Fed. Rep. Germany). N. Jb. Miner. Mh., 25–38.

LEAKE, B.E. (1978): Nomenclature of amphibole. Canadian Mineralogist, 16, 501–520.

LIATI, A. and MPOSKOS, E. (1990): Evolution of eclogites in the Rhodope Zone of Northern Greece. Lithos, 25, 89–99.

LIÉGEOIS, J.P. and DUCHESNE, J.C. (1981): The Lac Cornu retrograde eclogites (Aiguilles Rouges Massif, Western Alps, France): evidence of crustal origin and metasomatic alteration. Lithos, 14, 35–48.

LINDSLEY, D.H. (1983): Pyroxene thermometry. Amer. Mineral., 68, 477–493.

MARCHESI, M, MAZZUCCHELLI, M., BOTTAZZI, P., OTTOLINI, L. and VANNUCCI, R. (1992): Rocce subcrustali nella zona di Ivrea (Italia): i "corpi minori" della Val Strona. Atti Tic. Sc. Terra, 35 (note brevi 1992), 97–106.

MATTE, P. (1991): Accretionary history and crustal evolution of the Variscan belt. Tectonophysics, 196, 309–337.

MESSIGA, B. and BETTINI, E. (1990): Reaction behaviour during kelyphite and symplectite formation: a case study of mafic granulites and eclogites from the Bohemian Massif. Eur. J. Mineral., 2, 125–144.

MILLER, CH. and THÖNI, M. (1995); Origin of eclogites from the Austroalpine Ötztal basement (Tyrol, Austria): geochemistry and Sm–Nd vs Rb–Sr isotope systematics. Chem. Geol., 122, 199–225.

MORIMOTO, N., FABRIÈS, J., FERGUSON, A.K., GINZBURG, I.V., ROSS, M., SEIFERT, F.A., ZUSSMAN, J., AOKI, K. and GOTTARDI, G. (1988): Nomenclature of pyroxenes. Mineral. Mag., 52, 535–550.

MORTEN, L. (1987): Italy: a review of xenolithic occurrences and their comparison with Alpine peridotites. In: NIXON, P.H. (ed.): Mantle Xenoliths, J. Wiley and Sons Ltd, 135–148.

NICOLLET, C., LEYRELOUP, A. and DUPUY, J. (1979): Petrogenesis of high pressure trondhjemitic layers in eclogites and amphibolites from southern Massif Central, France. In: BARKER, F. (ed.): Trondhjemites, dacites, and related rocks, Elsevier, 435–463.

OTTEN, M.T. (1984): The origin of brown hornblende in the Artfjialet gabbro. Contrib. Mineral. Petrol., 86, 189–199.

OTTONELLO, G., ERNST, W.G. and JORON, J.L. (1984): Rare earth and 3d transition element geochemistry of peridotitic rocks: I. Peridotites from the Western Alps. J. Petrol., 25, 343–372.

PAQUETTE, J.L. (1987): Comportement des systèmes isotopiques U–Pb et Sm–Nd dans le métamorphisme éclogitique. Chaîne hercynienne et chaîne alpine. Thèse Univ. Rennes, 222 pp.

PEUCAT, J.J. (1986): Rb–Sr, U–Pb dating of the blueschists of the Ile de Groix. Geol. Soc. Mem., 164, 229–238.

PICCARDO, G.B., RAMPONE, E. and VANNUCCI, R. (1992): Evolution of mantle peridotites during passive continental rifting; examples from ancient and present situations. In: QUICK, J.E. and SINIGOI, S. (eds): Ivrea-Verbano Zone Workshop, U.S. Geol. Survey Circular, 11–12.

PIN, C. and VIELZEUF, D. (1988): Les granulites the haute pression d'Europe moyenne, témoins d'une subduction eo-hercynienne Bull. Soc. Géol. Fr., 8, 13–20.

PLYUSNINA, L.P. (1982): Geothermometry and geobarometry of plagioclase-hornblende bearing assemblages. Contrib. Mineral. Petrol., 80, 140–146.

RIVALENTI, G., GARUTI, G. and ROSSI, A. (1975): The origin of the Ivrea-Verbano basic formation (western Italian Alps): Whole rock geochemistry. Boll. Soc. Geol. Ital., 94, 1149–1186.

RIVALENTI, G., GARUTI, G., ROSSI, A., SIENA, F. and SINIGOI, S. (1980): Existence of different peridotite types and of a layered igneous complex in the Ivrea Zone of the Western Alps. J. Petrol., 22(1), 127–153.

SANTALLIER, D.S. (1983): Les eclogites du Bas-Limousin, Massif Central Français. Comportement des clinopyroxènes et des plagioclases antérieurement à l'amphibolitisation. Bull. Minéral., 106, 691–707.

SANTALLIER, D., BRIAND, B., MENOT, R.P. and PIBOULE, M. (1988): Les complexes leptyno-amphibolitiques (CLA): revue critique et suggestions pour un meilleur emploi du terme. Bull. Soc. Géol. Fr., 8, 3–12.

SPICHER, A. (1940): Geologie und Petrographie des oberen Val d'Isone (südliches Tessin). Schweiz. Mineral. Petrogr. Mitt., 20, 17–100.

SUEN, C.J. and FREY, F.A. (1987): Origins of the mafic and ultramafic rocks in the Ronda peridotite. Earth Planet. Sci. Lett., 85, 186–202.

SUN, S.S. and MCDONOUGH, W.F. (1989): Chemical and isotopic systematic of ocean basalts: implications for mantle composition and processes. In: SAUNDERS, A.D. and NORRY, M.J. (eds): "Magmatism in the Ocean Basins", Geol. Soc. Spec. Publ., 42, 313–345.

VAVRA, G., GEBAUER, D., SCHMID, R. and COMPTON, W. (1996): The multiple zircon growth and recrystallization during poliphase, Late Carboniferous to Triassic metamorphism in granulites of the Ivrea Zone (Southern Alps): an ion microprobe (SHRIMP) study. Contrib. Mineral. Petrol., 122, 337–358.

VON RAUMER, J.F. (1984): The Hercynian basement in the Helvetic realm, western and central Alps. Mem. Soc. Geol. It., 29, 57–69.

VOSHAGE, H., HOFMANN, A.W., MAZZUCCHELLI, M., RIVALENTI, G., SINIGOI, S., RACZEK, I. and DEMARCHI, G. (1990): Isotopic evidence from the Ivrea zone for a hybrid lower crust formed by magmatic underplating. Nature, 347, 731–736.

WELLS, P.R.A. (1977): Pyroxene thermometry in simple and complex systems. Contrib. Mineral. Petrol., 62, 129–139.

WILKINSON, J.F.G. and BINNS, R.A. (1977): Relatively iron-rich lherzolite xenoliths of the Cr-diopside suite: a guide to the primary nature of anorogenic tholeiitic andesite magmas. Contrib. Mineral. Petrol., 65, 199–212.

WOOD, B.J. and BANNO, S. (1973): Garnet-orthopyroxene and orthopyroxene-clinopyroxene relationships in simple and complex systems. Contrib. Mineral. Petrol., 42, 109–124.

Manuscript received December 5, 1996; revised manuscript accepted May 10, 1997.